REPORT DOCUMENTATION PAGE

Form Approved
OMB No. 0704-0188

PLEASE DO NOT RETURN YOUR FORM TO THE ABOVE ORGANIZATION.

1. REPORT DATE *(DD-MM-YYYY)*	2. REPORT TYPE	3. DATES COVERED *(From - To)*
14 MAY 2007	FINAL REPORT	01 JUL 03 - 31 DEC 06

4. TITLE AND SUBTITLE
BIOHAZARD DETOXIFICATION METHODS UTILIZING MAGNETIC PARTICLES

5a. CONTRACT NUMBER

5b. GRANT NUMBER
F49620-03-1-0403

5c. PROGRAM ELEMENT NUMBER

6. AUTHOR(S)
DR AXEL J. ROSENGART

5d. PROJECT NUMBER

5e. TASK NUMBER

5f. WORK UNIT NUMBER

7. PERFORMING ORGANIZATION NAME(S) AND ADDRESS(ES)
THE UNIVERSITY OF CHICAGO MEDICAL CENTER
DEPARTMENT OF NEUROLOGY AND SURGERY (NEUROSURGERY)
5758 S. MARYLAND AVENUE, CHICAGO, IL 60637

8. PERFORMING ORGANIZATION REPORT NUMBER

9. SPONSORING/MONITORING AGENCY NAME(S) AND ADDRESS(ES)
AFOSR/NL
875 NORTH RANDOLPH STREET
SUITE 325, ROOM 3112
ARLINGTON, VA 2203-1768
Dr Hugh Delong

10. SPONSOR/MONITOR'S ACRONYM(S)

11. SPONSOR/MONITOR'S REPORT NUMBER(S)

12. DISTRIBUTION/AVAILABILITY STATEMENT
APPROVE FOR PUBLIC RELEASE, DISTRIBUTION UNLIMITED.

AFRL-SR-AR-TR-07-0155

13. SUPPLEMENTARY NOTES

14. ABSTRACT

We are developing a novel, integrated system based on superparamagnetic, biocompatible nanospheres for selective and rapid detoxification of biological, chemical, or radioactive toxins from humans. After intravascular injection, the circulating nanospheres would bind to blood-borne toxins due to selective receptors attached to the nanosphere surface. After circulation, a suitable artery or vein is accessed with a small, hand held magnetic filter unit. The blood is purified of the toxin-loaded nanospheres within the unit and the clean blood is returned to the body. The concentrated toxins can now be disposed or submitted for assay or forensics. At the end of the funding period we have accomplished several key technological goals. A) We have a reporducible procedure for producing PEGylated PLGA/PLA nanospheres of discrete size in a range of 100 nm to 500 nm. We have finalized and are in the process of publishing our in vitro work which identifies the biocompatibility and non-toxicity of the designer spheres. B) Further, we have developed a prototype magnetic separator suitable for ambulatory usage and tested its performance in in vitro flow models.

15. SUBJECT TERMS

16. SECURITY CLASSIFICATION OF:			17. LIMITATION OF ABSTRACT	18. NUMBER OF PAGES	19a. NAME OF RESPONSIBLE PERSON
a. REPORT	b. ABSTRACT	c. THIS PAGE			19b. TELEPHONE NUMBER *(Include area code)*

2006 Performance Report for

BIOHAZARD DETOXIFICATION METHOD UTILIZING MAGNETIC PARTICLES

Agreement Number: P-03016

Submitted by

Dr. Axel J. Rosengart

Department of Neurology and Surgery (Neurosurgery)

The University of Chicago Medical Center

5758 S. Maryland Avenue

Chicago, IL 60637

and

Dr. Michael D. Kaminski

Process Chemistry and Engineering Department

Chemical Technology Division

Argonne National Laboratory

9700 S. Cass Avenue

Argonne, IL 60439

Submitted to

Dr. Hugh C. De Long

Program Manager, Biomimetics, Biomaterials, and Biointerfacial Sciences

Air Force Office of Scientific Research

Directorate of Chemistry and Life Sciences

4015 Wilson Blvd, Room 713

Arlington, VA 22203-1954

May 2007

OUTLINE

1. Objectives

The objectives of this work remain unchanged: to develop a portable, rapid detoxification system for blood-borne biological toxins. To do so, we are 1) designing, synthesizing and testing biodegradable magnetic nanospheres that have surface receptors with high affinity for the target biological toxin, and 2) designing, fabricating, and testing a prototype magnetic filter to separate the magnetic nanospheres from the blood.

2. Overall Aim and Status of Effort

We are developing a novel, integrated system based on superparamagnetic, biocompatible nanospheres for selective and rapid detoxification of biological, chemical, or radioactive toxins from humans. After intravascular injection, the circulating nanospheres would bind to blood-borne toxins due to selective receptors attached to the nanosphere surface. After circulation, a suitable artery or vein is accessed with a small, hand held magnetic filter unit. The blood is purified of the toxin-loaded nanospheres within the unit and the clean blood is returned to the body. The concentrated toxins can now be disposed or submitted for assay or forensics.

At the end of the funding period we have accomplished several key technological goals. A) We have a reproducible procedure for producing PEGylated PLGA/PLA nanospheres of discrete size in a range of 100 nm to 500 nm. We have finalized and are in the process of publishing our *in vitro* work which identifies the biocompatibility and non-toxicity of the designer spheres. B) Further, we have developed a prototype magnetic separator suitable for ambulatory usage and tested its performance in *in vitro* flow models.

3. Accomplishments –Period 2006/Early 2007

This section will present research highlights for the project, "Biohazard detoxification method utilizing magnetic particles," and the relationship of the research highlights to the

projects' goals. The significance of this research to the biomedical field, the relevance of this research to the Air Force's (AF's) mission, and potential applications of this research to the AF and civilian technology challenges will also be covered.

3.1. Research Highlights

We made significant progress in the development of high magnetization nanophases (Supplement I: Preparation and Characterization of Hydrophobic Superparamagnetic Magnetite Gel) and the development of magnetic PEGylated PLGA/PLA nanophases with suitable characteristics for future in vivo employment (Supplement II: Synthesis and Characterization of Highly-Magnetic Biodegradable Poly(D,L lactide-co-glycolide) Nanospheres).

Further, we expanded our in vitro flow models to validate the mathematical modeling (Supplement III: Theoretical analysis of a simple yet efficient portable magnetic separator design for separation of magnetic nano/micro-carriers from human blood flow) but also we enhanced our mathematical modeling capabilities to 3D simulations to better predict and optimize the performance of the magnetic separator device (Supplement IV: 3-Dimensional Modeling of A Portable Medical Device for Magnetic Separation of Particles from Biological Fluids and Supplement V: A parametric study of a portable magnetic separator for separation of nanospheres from circulatory systems). In addition, we tested prototype nanospheres and their substrates in an extensive *in vitro* biocompatibility battery which includes not several subforms of in vivo activation (and defense) mechanisms but also toxicological studies (Supplement VI: A comprehensive test battery for the in vitro biocompatibility assessment of nanocarriers for medical applications).

3.1.1. Supplement I:

Preparation and Characterization of Hydrophobic Superparamagnetic Magnetite Gel

Abstract

This study deals with the preparation and analysis of highly concentrated, hydrophobic oleic acid-coated magnetite gel. By contrast to conventional techniques to prepare magnetic fluid, herein the oleic acid was introduced as a reactant during the initial crystallization phase of magnetite which was obtained by the co-precipitation of Fe(II) and Fe(III) salts by addition of ammonium hydroxide. The resulting gelatinous hydrophobic magnetite was characterized in terms of morphology, particle size, magnetic properties, and crystal structure. The magnetic gel exhibited superparamagnetism at room temperature and could be well dispersed both in polar and nonpolar carrier liquids.

3.1.2. Supplement II:

Synthesis and Characterization of Highly-Magnetic Biodegradable Poly(D,L lactide-co-glycolide) Nanospheres

Abstract

The objective of this study was to develop high magnetization, biodegradable/biocompatible polymer-coated magnetic nanospheres for biomedical applications. Magnetic spheres were prepared by a modified single oil-in-water emulsion-solvent evaporation method utilizing highly-concentrated hydrophobic magnetite and poly(D,L lactide-co-glycolide) (PLGA). Hydrophobic magnetite prepared using oleic acid exhibited high magnetite concentrations (84 wt%) and good miscibility with biopolymer solvents to form a stable oily suspension. The oily suspension was then emulsified within an aqueous solution containing poly(vinyl alcohol). After rapid evaporation of the organic solvent, we obtained solid magnetic nanospheres. We characterized these spheres in terms of external morphology, microstructure, size and zeta potential, magnetite content and distribution within the nanospheres, and magnetic properties. The results showed good encapsulation where the magnetite distorted the smooth surface morphology only at the highest magnetite concentrations. The mean

diameter was 360-370 nm with polydispersity indices of 0.12-0.20, high magnetite content (40-60%) and high magnetization (26-40 emu/g). The high magnetization properties were obtained while leaving sufficient polymer to retain drugs making these biodegradable spheres suitable as a potential platform for the design of magnetically-guided drug delivery and other in vivo biomagnetic applications.

3.1.3. Supplement III:

Theoretical analysis of a simple yet efficient portable magnetic separator design for separation of magnetic nano/micro-carriers from human blood flow

Abstract

A technology that could physically remove substances from the blood such as biological, chemical, or radiological toxins could dramatically improve treatment of disease. One method in development proposes to use magnetic-polymer spheres to selectively bind toxins and remove them by magnetic filtration. Although magnetic filtration is a developed technology, the clinical boundary conditions described here require a new filter design. We investigated the removal of toxin-bound magnetic carriers from the bloodstream using 2-D FEMLAB simulations. The magnetic separator consisted of a permanent magnet with parallel ferromagnetic prisms on the faces and in contact with a straight tube carrying the magnetic-polymer spheres in suspension. We varied the following parameters: blood flow velocity, the size and number of ferromagnetic prisms and the ferromagnetic material in the both prisms and magnets. The capture efficiency reached maximum values when the depth of the prisms equaled the diameter of the tubing and the saturation magnetization of the prism material equaled twice that of the magnet. With this design a piece of 2 mm (diameter) tube carrying the fluid resulted in 95% capture of 2.0 m magnetic-polymer spheres at 10 cm/s flow velocity.

3.1.4. Supplement IV:

3-Dimensional Modeling of A Portable Medical Device for Magnetic Separation of Particles from Biological Fluids

Abstract

Our group is developing a detoxification system for the human blood that is based on magnetic nanoparticles. A key component of the proposed system is a portable magnetic filter that is capable of separating magnetic nanospheres from arterial blood flow in an extracorporeal unit. Since the objective is to minimize the time the patient is connected to the filter, we need to develop a filter that is capable of quantitative separation in potentially high-flow regimes. The design is to obtain an arterial puncture with a catheter, and pass the blood directly into a portable separator. In the separator design, an array of biocompatible capillary tubing and magnetizable wires is immersed in an external magnetic field that is generated by two permanent magnets. The wires are magnetized and the high magnetic field gradient from the magnetized wires helps to collect blood-borne magnetic nanospheres from blood flow. In this study, a 3-D numerical model was created and the effect of tubing-wire configurations on the capture efficiency of the system was analyzed using COMSOL Multiphysics 3.3®. The results showed that the configuration characterized by bi-directionally alternating wires and tubes was optimal. Preliminary in vitro experiments verified the numerical predictions. The results helped us optimize a prototype portable magnetic separator that is suitable for rapid sequestration of magnetic nanospheres from the human blood stream while accommodating necessary clinical boundary conditions.

3.1.5. Supplement V:

A parametric study of a portable magnetic separator for separation of nanospheres from circulatory systems

Abstract

A portable magnetic separator was proposed for in-vivo biomedical applications. In this prototype design, a matrix of alternating, parallel magnetizable wires and biocompatible tubing is immersed into an externally applied magnetic field. The wires are magnetized and high magnetic fields as well as field gradients are created to trap blood-borne flowing magnetic nanospheres in the tubing. In this paper, a parametric

investigation was carried out to evaluate the capture efficiency of flowing magnetic nanospheres by a separator unit consisting of single tubing and four wires. The parameters include: The mean blood velocity (1 to 20 cm/s); magnetic field strength (0.1 to 2.0 T); sphere size (500 nm to 1000 nm in radii); sphere magnetic material (iron, two types of magnetite) and magnetite content in the spheres (0.05 to 0.8 by weight); wire material (nickel, SS 430 and wairauite); wire length (2.0 to 20 cm); wire size (0.125 to 1.0 mm in radii); tubing size at a fixed ratio of tube to wire diameter of unity. The results showed that capture efficiencies of the spheres of well over 80% could easily be attained under reasonable human physiological conditions, provided that the mean blood velocities were below about 5.0 cm/s. The results also showed that the magnetic separator performance could be improved by maximizing the applied magnetic field strength up to about 1.0 T and decreasing the mean flow velocity in the tubing; by increasing the size of the spheres and their content of magnetic material; by utilizing magnetic materials in both the wires and the spheres with the highest magnetizations; by increasing the length of the separator; and by reducing the size of the unit with tubing and wires of equal radii. The results further optimize a prototype magnetic separator suitable for rapid sequestration of magnetic nanospheres from the human blood stream while accommodating necessary clinical boundary conditions.

3.1.6. Supplement VI:

A comprehensive test battery for the in vitro biocompatibility assessment of nanocarriers for medical applications

Abstract

Particles being considered for use as potential drug-carriers or agents involved in non-invasive stroke therapies, strict biological screening must be conducted to ensure the least immunological or cytotoxic bio-incompatibility. Our discussion focuses on the synthesis and characterization of biocompatible, magnetic PLGA-PEG microspheres intended for use in various biomedical applications. PLGA-based spheres, both nano and micrometers in size, were synthesized using standard oil-in-water emulsification method. A test battery including physico-chemical biocompatibility, immunological biocompatibility, and cell toxicity were compiled to achieve a comprehensive method in

the characterization and assessment of particles and/or other medically-feasible materials intended for such applications. Our group also describes the potential interactions and biological effects our particles present due to their physio-chemical characteristics as determined by biological assays.

4. Research Significance

Our aim is the introduction of a robust, hand-held, biodetection and treatment technology that can selectively detoxify human blood form target biohazards and furthermore, from provide a concentrated multi-analyte for high sensitivity bioassay. This proposed technology aims at establishing the ability to detoxify exposed humans from a wide variety of biological, chemical, and radiological (physical unrelated) toxic substances. Such a nanoscale platform technology can, in future efforts, be extended to achieve, among other applications: 1) portable in-field toxin identification, real-time monitoring, and quantitative detoxification in diverse scenarios of unknown exposures including civil and military sectors; 2) self- or helper application modus; 3) extension to unit or hospital-based detoxification centers; and 4) translated to other biomedical applications, for example, drug and medication overdose situations and chronic treatment of autoimmune illnesses. We strongly argue that our technology is designed to rather enhance and complement U.S. armament to effectively treat biohazards and not replace parallel efforts such as the development of novel antibiotics.

5. Publications - Participation and Presentations

1. M. Kaminski[1], H. Chen[2], Y. Xie[2], S. G. Guy[2] and A. Rosengart[2*] A Novel Human Detoxification System Based on Nanoscale Bioengineering and Magnetic Separation Techniques, accepted in Medical Hypothesis, 2005.
2. Y. Xie, M. D. Kaminski, C. J. Mertz, M. R. Finck, S. G. Guy, H. Chen, A. J. Rosengart. "Protein Encapsulated Magnetic Carriers for Micro/Nanoscale Drug Delivery Systems."

Proceedings of the 3rd Annual International IEEE EMBS Special Topic Conference on Microtechnologies in Medicine and Biology. Kahuku, Oahu, Hawaii, 162-165, 2005.

3. H. Chen, M. D. Kaminski, A. D. Ebner, J. A. Ritter, A. J. Rosengart. "Magnetizable Intravascular Stents for Sequestration of Systemically Circulating Magnetic Nano- and Microspheres," Proceedings of the 3rd Annual International IEEE EMBS Special Topic Conference on Microtechnologies in Medicine and Biology, Kahuku, Oahu, Hawaii, 286-289, 2005.
4. Axel J. Rosengart, Yumei Xie, Haitao Chen, and Michael D. Kaminski, "Magnetically Guided Plasminogen Activator-Loaded Designer Spheres for Acute Stroke Lysis," Med Hypotheses Res 2: 413-424, 2005.
5. A high gradient magnetic separator for separation of medicated magnetic submicrospheres from human arterial blood flow, Haitao Chen[1,5], Michael D. Kaminski[3], Armin D. Ebner[4], James A. Ritter[4], and Axel J. Rosengart, 50th magnetism and and magnetic material conference (Oct.30~Nov.3), journal of applied physics.
6. H. Chen, A. Ebner, M. D. Kaminski, A. J. Rosengart, J. Ritter, "Mathematical Modeling of Magnetic Filters and Stents as Medical Devices for Selective Separation or In Vivo Targeting of Functionalized Nanoparticles," Argonne National Laboratory Report ANL-CMT-04/02, September 2004.
7. M. D. Kaminski and A. J. Rosengart, "Detoxification of Blood using Injectable Magnetic Nanospheres: A Conceptual Technology Description," J. Magn. Magn. Mater., 293, 398-403, 2005.
8. M. D. Kaminski, A. J. Rosengart, Haitao Chen, Armin D. Ebner and James A. Ritter, "Magnetizable Intraluminal Stent and Functionalized Magnetic Carriers: A Novel Approach For Noninvasive Yet Targeted Drug Delivery," J. Magn. Magn. Mater., 293, 633–638, 2005.
9. C.J. Mertz, M.D. Kaminski, Y. Xie, M.R. Finck, S. Guy, and A.J. Rosengart, "In Vitro Studies of Functionalized Magnetic Nanoparticles for Selective Removal of a Simulant Biotoxin," J. Magn. Magn. Mater., 293, 572-577, 2005.
10. H. Chen, A. D. Ebner, J. A. Ritter, M. D. Kaminski, and A. J. Rosengart, "Analysis of Magnetic Drug Carrier Particle Capture by a Magnetizable Intravascular Stent. Part 3: Effect of Stent Design Parameters," accepted JMMM, 2004.

11. H. Chen, A. D. Ebner, M. D. Kaminski, A.l J. Rosengart, and James A. Ritter, "Analysis of magnetic drug carrier particle capture by a magnetizable intravascular stent-2: Parametric study with multi-wire two-dimensional model," J. Magn. Magn. Mater., 293, 616-632, 2005.
12. M. Aviles, A. D. Ebner, H. Chen, A. J. Rosengart, M. D. Kaminski, and J. A. Ritter, "Theoretical Analysis of a Transdermal Ferromagnetic Implant for Retention of Magnetic Drug Carrier Particles," J. Magn. Magn. Mater., 293, 605-615, 2005.
13. M. D. Kaminski and A. J. Rosengart, "Decorporation of Biohazards Utilizing Nanoscale Magnetic Carrier Systems," In: Nanofabrication Towards Biomedical Applications: Techniques, Tools, Applications, and Impact, C. S. S. R. Kumar, J. Hormes, and C. Leuschner (eds.), Wiley-VCH, Chapter 3.4, 442 pp.2004.
14. H. Chen, A. D. Ebner, A. J. Rosengart, M. D. Kaminski and J. A. Ritter, "Analysis of Magnetic Drug Carrier Particle Capture by a Magnetizable Intravascular Stent:1. Parametric Study with Single Wire Correlation," J. of Magnetism and Magnetic Materials, 284, 181-194, 2004
15. Haitao Chen, Patricia L. Caviness, Michael D. Kaminski, Armin D. Ebner, James A. Ritter, Sandra G. Guy1, Axel J. Rosengart, "Prototype Designs Of Portable Magnetic Separators For Extracorporeal Detoxification," Biomedical Engineering Society BMES 2005 Annual Meeting, Hyatt Regency, Baltimore, MD; Sep 28 -Oct 1, 2005.
16. "Development of a Magnetic Separator for Sequestration of Magnetic Micro Spheres Designed for Ex-Vivo Blood Detoxification" Separations Division submission for 2005 Annual Meeting (Cincinnati, OH)
17. M.D. Kaminski and A. J. Rosengart, "Nanotechnology-Based Detoxification For Internal Biohazard Exposures," 3rd annual Nano Materials for Defense Applications Symposium, Kona, HI, Feb. 21-25, 2005.
18. Haitao Chen[1,3], Michael D. Kaminski[2,5], Armin D. Ebner[4], James A. Ritter[4], Axel J. Rosengart, "Magnetizable Intravascular Stents for Sequestration of Systemically Circulating Magnetic Drug Carriers," submitted to 3rd Annual International IEEE-EMBS Special Topics Conference on Microtechnologies in Medicine and Biology, May 12-15, 2005, Turtle Bay Resort, Oahu, Hawaii.
19. Several presentations in Asia on medical applications of nanospheres.

20. M. Kaminski, Nanospheres in Medicine," presented at the Womens in Science Conference at Argonne National Laboratory, March 2005.
21. Haitao Chen, Patricia L. Caviness, Axel J. Rosengart, Michael D. Kaminski, Viji Balasubramanian, Armin D. Ebner, Sandra G. Guy, James A. Ritter Sequestration of Blood Borne Magnetic Drug Carrier Particles with Magnetizable Intravascular Stents," to be presented at the Biomedical Engineering: New Challenges for the Future, Biomedical Engineering Society, Wyndham Philadelphia at Franklin Plaza Philadelphia, Pennsylvania, October 13-16, 2004.
22. Yumei Xie, Michael D. Kaminski, Carol J. Mertz, Martha R. Finck, Sandra G. Guy, Viji Balasubramanian, Axel J. Rosengart, "Towards Plasminogen Activator Medicated Microspheres For Magnetically Guided Thrombolysis: Encapsulation Of Model Protein --- Bovine Serum Albumin," Biomedical Engineering: New Challenges for the Future, Biomedical Engineering Society, Wyndham Philadelphia at Franklin Plaza Philadelphia, Pennsylvania, October 13-16, 2004.
23. Yumei Xie, Michael D. Kaminski, Carol J. Mertz, Martha R. Finck, Vivian S. Sullivan, Sandra G. Guy, Axel J. Rosengart, Viji Balasubramanian, "The Effects Of Synthesis Conditions On The Surface Characteristics Of Biodegradable Microspheres," Biomedical Engineering: New Challenges for the Future, Biomedical Engineering Society, Wyndham Philadelphia at Franklin Plaza Philadelphia, Pennsylvania, October 13-16, 2004.
24. Kaminski MD, Rosengart AJ: Detoxification of blood using injectable magnetic nanospheres: A conceptual technology description. Journal of Magnetism and Magnetic Materials 2005 (May); 293(1): 398-403.
25. Mertz CJ, Kaminski MD, Xie Y, Finck MR, Guy SG, Rosengart AJ: In vitro studies of functionalized magnetic nanospheres for selective removal of a simulant biotoxin. Journal of Magnetism and Magnetic Materials 2005 (May); 293(1): 572-577.
26. Aviles M, Ebner A, Chen H, Kaminski MD, Rosengart AJ, Ritter J: Theoretical analysis of transdermal ferromagnetic implants for retention, retrieval, and guidance of magnetic drug carrier particles. Journal of Magnetism and Magnetic Materials 2005 (May); 293(1): 605-615.

27. Chen H, Ebner A, Rosengart AJ, Kaminski MD, Ritter J: Analysis of magnetic drug carrier particle capture by a magnetizable intravascular stent:-- 2: Effect of non-stent system parameters. Journal of Magnetism and Magnetic Materials 2005 (May); 293(1): 616-632.
28. Rosengart AJ, Kaminski MD, Chen H, Caviness PL, Ebner AD, Ritter JA: Magnetizable implants and functionalized magnetic carriers: a novel approach for noninvasive yet targeted drug delivery. Journal of Magnetism and Magnetic Materials 2005 (May); 293(1): 633-638.
29. Rosengart AJ, Xie Y, Chen H, Kaminski MD: Magnetically guided plasminogen activator-loaded designer spheres for acute stroke lysis. Medical Hypothesis and Research 2005 (July); 2(3): 413-424
30. Xie Y, Kaminski MD, Guy SG, Rosengart AJ: Plasminogen activator loaded magnetic nanocarriers for stroke therapy: a mass balance feasibility evaluation. Journal of Biomedical Nanotechnology 2005; 1(4):410-415.
31. Xie Y, Kaminski MD, Mertz CJ, Finck MR, Guy SG, Chen H, Rosengart AJ: Protein encapsulated magnetic carriers for micro/nanoscale drug delivery systems. In: Proceedings of the 3rd Annual International IEEE EMBS Special Topic, Conference on Microtechnologies in Medicine and Biology; 2005, May 12-15; Oahu, HI. Washington: Institute of Electrical and Electronics Engineers; 2005.
32. Liu X, Kaminski MD, Guan Y, Chen H, Liu H, Rosengart AJ: Preparation and characterization of hydrophobie superparamagnstic magnetite gel. Journal of Magnetism and Magnetic Materials 2006; 306: 248-253
33. Chen H, Kaminski MD, Caviness PL, Xianqiao L, Dhar P, Torno M, Rosengart AJ: Magnetic separation of microspheres from viscous biological fluids. Physics in Medicine and Biology 52: (2007) 1185-1196
34. Chen H, Kaminski MD, Ebner AD, Ritter JA, Rosengart AJ: Theoretical analysis of a simple yet efficient portable magnetic separator design for separation of magnetic nano/micro-carriers from human blood flow. Journal of Magnetism and Magnetic Materials 2007: 313: 127-134
35. Liu X, Novosad V, Rozhkova E, Chen H, Yefremenko V, Person J, Torno M, Rosengart AJ: Surface Functionalized Biocompatible Magnetic Nanospheres for Cancer Hyperthermia. IEEE Transactions on Magnetics *(accepted)*

36. Chen H, Bockenfeld D, Rempfer D, Kaminski MD, Liu X, Rosengart AJ: Preliminary 3-D analysis of a high gradient magnetic separator for biomedical applications. Journal of Applied Physics (accepted)
37. Chen H, Kaminski MD, Lio X, Mertz CJ, Xie Y, Torno MD, Rosengart AJ: A novel human detoxification system based on nanoscale bioengineering and magnetic separation techniques. Medical Hypotheses 2007; 68:1071-1079
38. Aviles MO, Chen H, Ebner AD, Rosengart AJ, Kaminski MD, Ritter JA: In vitro study of a ferromagnetic stent for implant assisted-magnetic drug targeting. Journal of Magnetism and Magnetic Materials 2006;11: 156
39. Xie Y, Kaminski MD, Torno MD, Finck MR, Liu X, Rosengart AJ: Physicochemical characteristics of magnetic microspheres containing tissue plasminogen activator. Journal of Magnetism and Magnetic Materials 2006;11: 172
40. Chen H, Bockenfeld D, Rempfer D, Kaminski MD, Rosengart AJ: 3-dimensional mathematical modeling of a portable device for magnetic separation of nano/micro-spheres from biological fluids. (submitted)
41. Liu X, Kaminski MD, Chen H, Torno M, Taylor L, Rosengart AJ: Synthesis and characterization of highly-magnetic biodegradable poly (D,L-lactide-co-glycolide) nanaospheres. J Controlled Substance (accepted)
42. Chen H, Kaminski MD, Ebner AD, Ritter JA, Rosengart AJ: 2-D modeling and preliminary in-vitro investigation of a prototype high gradient magnetic separator for biomedical applications. Medical Engineering & Physicis. 2007 (accepted)
43. Liu X, Kaminski MD, Riffle JS, Chen H, Torno M, FInck MR, Taylor L, Rosengart AJ: Preparation and characterization of biodegradable magnetic carriers by single emulsion-solvent evaporation. Journal of Magnetism and Magnetic Materials 2006;10:1170

6. Consultative and Advisory Functions

This program has given us an opportunity to found a collaboration of single investigators at several institutions who share the same mission of developing nanotechnologies for medical applications. We have the following institutions involved:

Argonne National Laboratory, The University of Chicago, Illinois Institute of Technology, University of South Carolina, University of British Columbia, Case Western Reserve University, University of Western Australia, and Virginia Polytechnic Institute. We are using this collaboration to leverage additional funding, expand our experimental resources through in-kind effort, and expand our intellectual database for technology development.

3-Dimensional Modeling of A Portable Medical Device for Magnetic Separation of Particles from Biological Fluids

Haitao Chen[1,5], Danny Bockenfeld[3], Dietmar Rempfer[3], Michael D. Kaminski[4*], and Axel J. Rosengart[1,2*]

Departments of [1]Neurology and [2]Surgery (Neurosurgery), The University of Chicago Pritzker School of Medicine, Chicago, IL 60637, USA; [3]Department of Mechanical, Material and Aerospace Engineering, Illinois Institute of Technology, Chicago, IL 60616, USA; [4]Chemical Engineering Division, Argonne National Laboratory, Argonne, IL 60439, USA; [5]Department of Biomedical Engineering, Illinois Institute of Technology, Chicago, IL 60616, USA; [1-5]Collaborative Investigators for Applied Nanotechnology in Medicine

*Corresponding Authors
Axel J. Rosengart, M.D., Ph.D.
Michael D. Kaminski, Ph.D.
The University of Chicago Medical Center
5841 South Maryland Ave, MC 2030
Chicago, IL, 60637, USA
Tel: (773) 702-2364
Fax: (773) 834-4612
E-mail: arosenga@neurology.bsd.uchicago.edu

Abstract

Our group is developing a detoxification system for the human blood that is based on magnetic nanoparticles. A key component of the proposed system is a portable magnetic filter that is capable of separating magnetic nanospheres from arterial blood flow in an extracorporeal unit. Since the objective is to minimize the time the patient is connected to the filter, we need to develop a filter that is capable of quantitative separation in potentially high-flow regimes. The design is to obtain an arterial puncture with a catheter, and pass the blood directly into a portable separator. In the separator design, an array of biocompatible capillary tubing and magnetizable wires is immersed in an external magnetic field that is generated by two permanent magnets. The wires are magnetized and the high magnetic field gradient from the magnetized wires helps to collect blood-borne magnetic nanospheres from blood flow. In this study, a 3-D numerical model was created and the effect of tubing-wire configurations on the capture efficiency of the system was analyzed using COMSOL *Multiphysics* 3.3®. The results showed that the configuration characterized by bi-directionally alternating wires and tubes was optimal. Preliminary *in vitro* experiments verified the numerical predictions. The results helped us optimize a prototype portable magnetic separator that is suitable for rapid sequestration of magnetic nanospheres from the human blood stream while accommodating necessary clinical boundary conditions.

Keywords: Magnetic separation; magnetic nanospheres; high-gradient magnetic separation (HGMS); detoxification

1. Introduction

Current progress in biomedical engineering increasingly employs designer carrier molecules in animals and humans to successfully transport and deliver otherwise labile or harmful pharmacotherapeutics.[1-3] Even more, some nanocarrier designs allow the co-encapsulation of a drug of choice with superparamagnetic materials such as magnetite[9] to allow external magnetic fields to control or guide the carrier, even when circulating within the fast-flowing vasculature.[7,10,11] Examples for such drug delivery concepts include magnetically-aided delivery of the clot buster tissue plasminogen activator (tPA) for the reversal of acutely-occluded arteries in patients with acute stroke or heart attacks,[7] or the magnetically-supported delivery of cancer therapeutics to liver tumors or skin cancer.[12-13] In contrast to technologies which employ magnetic designer carriers for advanced drug systems, it is also of great medical interest if freely circulating nanocarriers could be removed selectively and quantitatively from the blood. For example, a novel therapeutic approach for detoxification of blood utilizes toxin-binding carriers to capture freely circulating toxins to their surface while subsequent *in vivo* magnetic separation removes the toxin-bound carrier complexes from the blood.[14] The selective and physical elimination (and not merely the binding and passive excretion over time) of blood-bound toxins, such as radionuclides, from the circulation could favorably decrease the injury-severity of accidentally and therapeutically exposed humans and would provide a platform technology for effective biohazard countermeasures. To this end, we have recently proposed and, in preliminary investigations, reported about a novel device, a magnetic separator, to remove magnetic carriers from the blood stream utilizing a minimally-invasive and medically-feasible approach (Fig.1).[15] However, many theoretical and practical questions with respect to the optimal bioengineering design of such a magnet separator for human applications remain open. The herein reported

research focuses on the theoretical analyses and optimization of a small, portable separator while employing important biomedical boundary conditions.

Magnetic separators for industrial or *in vitro* usages are not new and have been studied for several years;[16-18] however, real-time, magnetic separation in the living organism is distinct as it demands specific and precise design requirements with respect to the human physiology and its proposed medical applications. Different from the magnetic filters in other proposed magnetic extracorporeal units for removing medical agents from body fluids (Gordon *et al* 2003, Carew *et al* 1992), which focused on increasing the magnetic field strength in the separators and did not emphasize portability, the filter (Chen 2006a) in our system is designed around portability. Our preliminary analyses employed two-dimensional theoretical modeling to predict the feasibility of this prototype magnetic separator[15] which, in its basic design, consists of an array of alternating capillary tubing and magnetizable wires. The entire wire-tube unit is exposed to a magnetic field generated from two parallel, permanent magnets with the field oriented perpendicular to the wires and blood flow. The magnetic field gradients created by the magnetized wires permits the collection of the magnetic nanocarriers while the tubing channels blood along the wires at low flow rates. For human applications the device will receive and return blood from a peripheral (i.e., arm, leg) vascular access by simple dual-lumen cannulation to perfuse the device. The principle for the magnetic separator borrows from and combines two established technologies, the high gradient magnetic separation (HGMS) technique as practiced in industry, for example, for the separation of waste products,[19-21] and the biomedical use of extracorporeal blood circulation, which is the temporary removal and immediate return of blood from and back to the body such as used in hemodialysis for patients with failing kidneys.[22-24] However, in contrast to hemodialysis and similar clinical procedures, no direct blood manipulation is required in this

magnetic separation process; hence, the primary device features includes design strategies for ambulatory usage (i.e., light weight, zero power, etc.).[25]

However, it remains to be established what wire-tubing configuration will allow maximal retention of the magnetic carrier within a biomedical useful device. Optimizing this capture efficiency (CE) within the magnetic separator becomes especially important with respect to its potential future use as an ambulatory blood cleansing method suitable also for in-field application. In this paper, a three-dimensional theoretical model was established to analyze the effect of various wire-tube configurations (Fig.2) on the CE at various mean flow velocities and applied magnetic field intensities while accommodating necessary clinical boundary conditions. Preliminary *in vitro* experiments verified the numerical predictions. The results show that the geometric configuration characterized by bi-directionally alternating wires and tubes was optimal.

2. Model Development

Positioning the wires within the blood stream is not suitable for prospective biomedical applications due to the high risks of blood clotting induced by interactions between blood components and the wires themselves and also from the very high velocity gradients in the blood flow caused by the wire obstructions. However, to achieve the high magnetic field gradients required for effective separation, the wires must be fine and intimate to the blood flow. The proposed magnetic separator consists of a matrix of parallel biocompatible capillary tubing and fine magnetizable wires, which are immersed in an externally applied magnetic field.

The finite element package COMSOL Multiphysics 3.3® was used in order to numerically solve the three-dimensional partial differential equations that constitute the model,

and to predict the trajectories of the magnetic spheres as they travel with the blood from left to right through the tubing while under the influence of both hydrodynamic and magnetic forces. In order to reduce the complexity of the model, only one cell of each of the spatially periodic configurations (see Fig. 2) was used. Fig. 2a shows a central tube with wires in each of the cross-flow directions, a 4-wire (0) configuration, where "0" indicates the angle (in degree) between the applied magnetic field and one plane passing through the axes of tubing and the wires. The basic unit in Fig.2b also consists of four wires and one tube and is named 4-wire (45) configuration because the angle between the applied magnetic field and the wire-tubing-wire plane is 45°. The basic unit in Fig.2c is named 4-wire (Hexa) configuration in order to differ it from the others. Fig.2d shows the central tubing with a row of three wires above and below it, a 6-wire configuration. A representative three-dimensional control volume (CV) is provided (Fig. 3) for reference.

The methodology utilized here to determine the numerical CE, CE_{num}, is a 3-D extension of the 2-D methodology used in the previous study.[10] The simplicity of the model was achieved by considering only the hydrodynamic (due to the blood flow) and the magnetic forces (due to the effect of the external magnetic field and magnetized wires). Inertial and lift forces, as well as the magnetic interparticle forces that might lead to magnetic sphere agglomeration were neglected. The magnetic sphere trajectory ψ was determined from

$$\nabla \times \psi = \mathbf{u}_p, \tag{1}$$

where $\mathbf{u}_p$ represents the particle velocity. CE_{num} is given by

$$CE_{num} = 1 - \frac{n_{p,out}}{n_{p,in}}, \tag{2}$$

where $n_{p,in}$ is the chosen number of starting points for the magnetic sphere trajectories described by Eq. (1), and $n_{p,out}$ is the number of trajectories which exit the tubing.

To evaluate Eq. (1), however, the variables that help determine $\mathbf{u}_p$ must be evaluated first. This can be done by resolving the force balance that includes hydrodynamic and magnetic forces upon a single magnetic sphere everywhere inside the tubing. These two types of forces were independently evaluated as follows. We first found the blood velocity (υ_x, υ_y, υ_z) and the blood pressure **P** within the tubing by solving the continuity and 3-D Navier-Stokes equations for blood, which was assumed to be an incompressible fluid of density ρ_B and viscosity η_B,

$$\nabla \cdot \mathbf{u} = 0 \tag{3}$$

$$\rho_B \left[\frac{\partial \mathbf{u}}{\partial t} + (\nabla \mathbf{u}) \cdot \mathbf{u} \right] = -\nabla \mathbf{P} + \eta_B \nabla^2 \cdot \mathbf{u} \tag{4}$$

The blood flow velocity was assumed to enter the tubing at $z = 0$ in a direction parallel to the tubing walls (i.e., $u_x = 0$ and $u_y = 0$) and with parabolic profile with average velocity U_o. At the wall of the tubing, the velocity in all directions is identically zero and at the outlet of the tubing the blood pressure was specified as $\mathbf{P_o}$=1 atm.

Next, the magnetic force upon the magnetic sphere was determined by evaluating the magnetic field **H** within the CV. This was done using the Maxwell equation within the CV

$$\nabla^2 \varphi = 0, \tag{5}$$

where φ is the scalar magnetic potential and is related to the field **H** according to:

$$\mathbf{H} = -\nabla \varphi . \tag{6}$$

However, the system was composed of two regions with very distinct magnetic behavior. The first region corresponded to the non-magnetic space not occupied by wires; the second region corresponded to the space occupied by the wires, which was magnetizable in the presence

of an external magnetic field. The discrete nature of the system required that the magnetic potential be defined differently for each of the regions as φ_1, and φ_2, respectively. Thus, the Maxwell equation was redefined as

$$\nabla^2 \varphi_1 = 0, \tag{7a}$$

$$\nabla^2 \varphi_2 = 0, \tag{7b}$$

with the respective **H** being

$$\mathbf{H_1} = \left(H_{1,x}, H_{1,y}, H_{1,z}\right) = \left(-\frac{\partial \varphi_1}{\partial x}, -\frac{\partial \varphi_1}{\partial y} + H_o, -\frac{\partial \varphi_1}{\partial z}\right), \tag{8a}$$

$$\mathbf{H_2} = \left(H_{2,x}, H_{2,y}, H_{2,z}\right) = \left(-\frac{\partial \varphi_2}{\partial x}, -\frac{\partial \varphi_2}{\partial y} + H_o, -\frac{\partial \varphi_2}{\partial z}\right). \tag{8b}$$

On the other hand, the respective magnetic fluxes were defined as

$$\mathbf{B_1} = \mu_o (H_{1,x}, H_{1,y}, H_{1,z}) = \mu_o \left(-\frac{\partial \varphi_1}{\partial x}, -\frac{\partial \varphi_1}{\partial y} + H_o, -\frac{\partial \varphi_1}{\partial z}\right), \tag{9a}$$

$$\begin{aligned} \mathbf{B_2} &= \mu_o (H_{2,x}, H_{2,y} + M_w, H_{2,z}) \\ &= \mu_o \left(-\frac{\partial \varphi_2}{\partial x}, -\frac{\partial \varphi_2}{\partial y} + H_o + M_w, -\frac{\partial \varphi_2}{\partial z}\right), \end{aligned} \tag{9b}$$

where M_w corresponds to the magnetization in the wires (i.e., region 2). This magnetization was assumed parallel to $\mathbf{H_1}$ and their relationship were defined as

$$\left|\mathbf{M}_w\right| = 2\alpha_w H_o, \tag{10a}$$

$$\alpha_w = \min\left(\frac{\chi_{w,o}}{2 + \chi_{w,o}}, \frac{M_{ws}}{2H_o}\right), \tag{10b}$$

where $\chi_{w,o}$ and M_{ws} are the magnetic susceptibility at zero magnetic field and the saturation magnetization of the wires, respectively.

To solve Eq. 7, continuity conditions were applied for the magnetic potential (i.e., φ_1, and φ_2) and the normal components of the magnetic fluxes (i.e., $\mathbf{B_{1,n}}$, and $\mathbf{B_{2,n}}$) at every interface between the two defined regions.

In addition, the CV was assumed sufficiently large to impose $\varphi_2 = 0$ along its boundaries. The following expression was then used to evaluate the magnetic force ($\mathbf{F_m}$) on a magnetic sphere:

$$\mathbf{F_m} = \frac{1}{2}\omega_{fm,p} V_p \mu_o \frac{M_{fm,p}}{H} \nabla(\mathbf{H_1} \cdot \mathbf{H_1}) \tag{11}$$

where μ_o is the magnetic permeability of vacuum, V_p is the volume of the magnetic spheres, and $\omega_{fm,p}$ and $M_{fm,p}$ are the volumetric fraction and magnetization of the ferromagnetic material in the magnetic spheres, respectively.

The magnetization of the material in the spheres $M_{fm,p}$ was assumed parallel to the field $\mathbf{H_1}$. Because the ferromagnetic material in each magnetic sphere was assumed to consist of fully dispersed, single domain, spherical magnetic particles of radius R_{sdp}, the relationship between the magnetization $M_{fm,p}$ and $\mathbf{H_1}$ was assumed to follow Langevin's law,

$$M_{fm,p} = M_{fm,s}\left[\coth\left(\frac{\mu_o M_{fm,s} V_{sdp}\left(H_1 - \frac{1}{3}\omega_{fm,p} M_{fm,p}\right)}{k_b T}\right) - \frac{k_b T}{\mu_o M_{fm,s} V_{sdp}\left(H_1 - \frac{1}{3}\omega_{fm.p} M_{fm,p}\right)}\right] \tag{12}$$

where $M_{fm,s}$ is the saturation magnetization of the ferromagnetic material inside the magnetic sphere, V_{sdp} is the volume of a single magnetic particle inside the sphere, k_b is the Boltzman constant and T is the absolute temperature. The term, $1/3\,\omega_{fm,p} M_{fm,p}$, accounts for the demagnetization field due to the magnetic sphere as a whole. For simplicity, however, this term

was neglected, mainly due to the small volume fraction $\omega_{fm,p}$ occupied by the ferromagnetic particles inside a magnetic sphere.

If $\rho_{fm,p}$ represents the density of the ferromagnetic material inside the magnetic sphere and $\rho_{pol,p}$ represents the density of the polymer and drug solution comprising the rest of the magnetic sphere, then

$$\omega_{fm,p} = \rho_p \frac{x_{fm,p}}{\rho_{fm,p}} \tag{13}$$

$$\rho_p = \frac{1}{\frac{x_{fm,p}}{\rho_{fm,p}} + \frac{1 - x_{fm,p}}{\rho_{pol,p}}} \tag{14}$$

With the expressions for the hydrodynamic forces,

$$\mathbf{F_d} = 6\pi\eta_B R_p(\mathbf{u} - \mathbf{u}_p), \tag{15}$$

and magnetic forces (Eq. 11) defined, Newton's second law of motion for a magnetic sphere, i.e., $\mathbf{F_m} + \mathbf{F_d} = 0$, was finally used to obtain an explicit expressions for the magnetic sphere velocity $\mathbf{u_p}$,

$$\mathbf{u_p} = \mathbf{u} + \frac{1}{9}\frac{\mu_o R_p^2 \omega_{fm,p}}{\eta_B}\frac{M_{fm,p}}{H_1}\nabla(\mathbf{H_1}\cdot\mathbf{H_1}), \tag{16}$$

which follows from equating the Stokes drag of our magnetic particle (Eq.15) with the magnetic force. The components of the magnetic sphere velocity are

$$\mathbf{u}_{\mathbf{p},x} = \mathbf{u_x} + \frac{V_m R_b}{U_o M_w H_1}\left(\frac{\partial\varphi_1}{\partial x}\frac{\partial^2\varphi_1}{\partial x^2} + \left(\frac{\partial\varphi_1}{\partial y} - H_o\right)\frac{\partial^2\varphi_1}{\partial x\partial y} + \frac{\partial\varphi_1}{\partial z}\frac{\partial^2\varphi_1}{\partial x\partial z}\right) \tag{17a}$$

$$\mathbf{u}_{\mathbf{p},y} = \mathbf{u_y} + \frac{V_m R_b}{U_o M_w H_1}\left(\frac{\partial\varphi_1}{\partial x}\frac{\partial^2\varphi_1}{\partial x\partial y} + \left(\frac{\partial\varphi_1}{\partial y} - H_o\right)\frac{\partial^2\varphi_1}{\partial y^2} + \frac{\partial\varphi_1}{\partial z}\frac{\partial^2\varphi_1}{\partial y\partial z}\right) \tag{17b}$$

$$\mathbf{u}_{\mathbf{p},z} = \mathbf{u}_{\mathbf{z}} + \frac{V_m R_b}{U_o M_w H_1}\left(\frac{\partial \varphi_1}{\partial x}\frac{\partial^2 \varphi_1}{\partial x \partial z} + \left(\frac{\partial \varphi_1}{\partial y} - H_o\right)\frac{\partial^2 \varphi_1}{\partial y \partial z} + \frac{\partial \varphi_1}{\partial z}\frac{\partial^2 \varphi_1}{\partial z^2}\right) \qquad (17c)$$

where V_m, the so-called magnetic velocity, is given by

$$V_m = \frac{1}{9}\frac{R_p^2}{R_b}\frac{\mu_o}{\eta_B}\omega_{fm,p} M_{fm,p.} M_w \qquad (18)$$

3. Materials and Methods

1.7 μm polystyrene (PS) magnetic spheres (saturation magnetization=10.65 emu/g) were purchased from Micromod GmbH (Rostock, Germany). Straight, stainless-steel type 430 wires (1.0 mm in diameter and 10 cm in length) with saturation magnetization=175 emu/g were purchased from California Fine Wire Company (Grover Beach, CA, USA). Capillary glass tubing (1.0 mm in outer diameter, 0.75 mm in inner diameter and 15 cm in length) was from World Precision Instruments, Inc. (Sarasota, FL, USA).

The magnetic separators consisted of a piece of capillary tubing and multiple pieces of stainless steel wires. A relatively homogenous external magnetic field was created by two parallel rectangular NdFeB magnets (4×4×1.25 inch; Magnet Sales & Manufacturing Inc., CA, USA). The magnetic field was measured by a 4048CE F.W.Bell Gaussmeter (Sypris Test and Measurement, FL, USA). The tubing-wire setup was sandwiched between the magnets and relatively high magnetic gradients were provided by the magnetized wires.

The experimental set-up consisted of a SP100I syringe pump (World Precision Instruments, Inc., FL, USA), a HGMS magnetic separator unit described above, and a receiving container (Fig.4). The syringe pump drove the sample suspension through the HGMS separator where a fraction of the magnetic spheres were collected against the tubing wall and the remaining drained into the receiving container.

Magnetic sphere sample suspensions (4 mg/100 ml, about $1.5x10^7$ spheres/ml) were prepared and 10 ml was used for each experimental run. In order to quantify the concentration of the spheres using turbidity measurement, we determined the correlation between the concentration and turbidity of the samples as follows. Original magnetic sphere sample suspension (50 mg/ml) 1 ml was lyophilized for a days. Then 0.05 mg/ml solution was prepared by dispersing the weighed dried solid spheres in deionized water. Serial dilution of the solution by a factor of two and the turbidity of the samples was measured by a 2100P portable turbidimeter from Hach Company (Loveland, CO). The concentration (C) - turbidity (T) correlation could be well-deduced by polynomial fitting of experimental data. The concentration of sphere solution (C) were calculated from turbidity of the sample using this nonlinear correlation as,

$$C = \frac{\sqrt{28.705^2 + 4 \times 5.7536 \times (T - 0.0773)} - 28.705}{2 \times 5.7536} \tag{19}$$

where T (in NTU) is the turbidity of the sample.

In order to compare the experimental results with the numerical results, we eliminated the contribution to CE from the capture of spheres by the two magnets alone (no wires), which usually can retain magnetic spheres at the inlet and outlet, where the field gradients of the magnets are large. Then, the CE of magnetic spheres was calculated using the following formula:

$$CE = \frac{CE_{exp} - CE_{control}}{1 - CE_{control}} \times 100\% \tag{20}$$

where CE_{exp} is the capture efficiency of the sample by the separation system including applied magnetic field. $CE_{control}$ is the capture efficiency of the sample by the applied magnetic field only. CE_{exp} and $CE_{control}$ were calculated from

$$CE\,\exp/control = \frac{C_{before} - C_{after}}{C_{before}} \times 100\% \qquad (21)$$

where C_{before} and C_{after} are the concentration of the sample before and after the collection, respectively. C_{before} and C_{after} was obtained via concentration-turbidity correlation (Eq.19) by the measurement of turbidity of the samples.

The parameters used in the model and the experiments are listed in Table 1.

4. Results and Discussion

We developed a 3-D numerical model to better simulate a portable, magnetic filter than can be done in 2-D (Chen 2007). The purpose of this work was to compute the capture efficiency of the filter for magnetic microparticles as a function of wire-tube configuration, fluid flow velocity, and magnetic field strength. These computations were then compared to experiment for agreement.

Before discussing CE_{num}, it is helpful to look at the trajectories to obtain an understanding of the particle movement. The trajectories differed dramatically between planes and between wire configurations (Fig. 5). Similarly, the trajectories in the x = 0 plane tended to move towards the wall of the tubing (Fig.5a1 and Fig.5b1), while the trajectories in the y = 0 plane tended to move away from the wall of the tubing (Fig.5a1 and Fig.5b1). However, in both planes, the deflection was stronger in the 4-wire (0) configuration than in the 6-wire configuration (Fig.5a), which qualitatively indicates that the 4-wire (0) configuration was a better design.

At low velocity (<2 cm/s), the CE was greater than 95% for all configurations (Fig. 6). As the velocity increased, the CE decreased significantly for the 4-wire (Hexa) and more rapidly for the 6-wire design. Clearly, the 4-wire (0) and 4-wire (45) designs produced superior CE, being >95% for the up to 10 cm/s, even though the magnetic fields set up by these two designs

differed dramatically (Fig. 6). In the 4-wire (0) design, the wires created high values of the magnetic field in the y-direction, while in the 4-wire (45) design the wires created high fields in the x-direction and there was strong coupling between the magnetic fields of the wires (visualized as the continuous red regions in the y-direction and the continuous blue in the x-direction). This tells us that, with regard to CE, the direction of the applied magnetic field is not an important factor in the 4-wire (0) configuration if the applied magnetic field is perpendicular to the flow. The relative position between the wires and the tube is what matters.

By adjoining the wires in the 4-wire (Hexa) and 6-wire designs, the magnetic field lines became smoother (Fig. 6), thereby reducing the field gradients and the CE over the other 4-wire configurations. The reduced CE occurred despite the significant increase in the value of the magnetic field in the 4-wire (Hexa) and 6-wire configurations (noted by the yellow in the flow tube region). These data highlight the importance of the magnetic field gradient in particle capture. In the 4-wire (0) and (45) configurations, the value of the magnetic field is low but the field gradients must be high in order to effect the large CE that was calculated. In the 4-wire (Hexa) and 6-wire designs, the strong magnetic field could not offset the concomitant decrease in the magnetic field gradients set up by the adjoining wires.

Another design that warrants brief mention is a 6-wire hexagonal configuration, where the central tubing is surrounded by six adjacent wires (Fig 9). As with the 4-wire (Hexa) and 6-wire configurations, the magnetic field is strong in the flow tube region but the field gradients is low. Unfortunately, the numerical model presented in this paper could not accurately determine the capture efficiency for the hexagonal configuration; we believe that the inaccuracy resides with the method by which the model treats the proximity of the poles of the magnetized wires to one another. Physically, the magnetic field of one wire would influence the magnetic field in

another. However, experiments revealed that the 6-wire hexagonal configuration produced the lowest CE of all the configurations tested (data not shown).

Increasing the external magnetic field while holding the mean blood flow velocity constant (here U_o = 5 cm/s) increased the CE, as expected (Fig. 7). This effect was due to an increase in the magnetization of the wires and an increase in the external magnetic field. The CE also followed the same sequence as in Fig.6.

The numerical computation of the CE was in good agreement with the experimental data up to 20 cm/s (Fig.6). At 20 cm/s, the values deviated from each other because we did not include the effect of shear forces, which become more important at high velocity. Despite that, the model and experiments produced the same CE sequence and similar trend when the applied field increased from 0.05 T to 0.5 T (Fig.7). The experimental results were larger than the corresponding numerical results at low applied magnetic field strength, for example, 0.05 T. This may be due to the crude expression of the wire magnetization (Eq.11) used in the model. Though it is a traditional formula for the magnetization of a cylindrical wire in an applied magnetic field, it is not able to accurately reflect the magnetization of a wire. This was evidenced by vibrating sample magnetometry (data not shown), which showed faster magnetization than that expressed by Eq. 11. A smoother approximation of wire magnetization may improve the accuracy of the model at low flow rates.

Of note, the 4-wire (0) design was geometrically similar to conventional quadrupole magnetic field designs (Fig.8). However, the two poles along the y-direction in the 4-wire (0) configuration (Fig.8a) are attractive while the poles in a quadrupole design (Fig.8a) produce opposing magnetic field lines and repel each other along both x-direction and y-direction.

Consequently, the magnetic fields, as well as resulting magnetic forces in the two designs, are quite different.

The results from the model fit well with the data from *in vitro* flow experiments (Figs.6-7). However, the relatively large discrepancy at high flow velocity ($\geq$ 20 cm/s) and low applied magnetic field strength ($\leq$ 0.3 T) necessitates further improvement of the model by including factors such as shear forces as well as sphere agglomeration. Moreover, a more realistic expression of wire magnetization may also be important. One might question the validity of using a single control volume to describe the magnetic field and extrapolating that to a multiple tubing device. Rigorously, for a multiple tubing device we would invoke periodic boundary conditions to more accurately describe the filter, but we did not observe any noticeable difference between the data from the model when periodic boundary conditions were included and the model as described herein (data not shown).

5. Conclusion

A 3-D numerical model was developed to evaluate the capture of magnetic spheres by a prototype, portable magnetic separator consisting of an array of biocompatible capillary tubing and ferromagnetic wires immersed in an external magnetic field. In the configurations investigated, the design with four wires equidistantly surrounding the flow tube had much higher capture efficiency than the configurations consisting of adjoining wires. The external field direction was not an important factor in the two designs, if it was aligned perpendicular to the flow. Preliminary *in vitro* experiments verified the numerical predictions at low flow velocity (<20 cm/s) and high applied magnetic field (>0.3 T). Outside this range, the model deviated from the experiment because the model lacks sufficient detail to account for shear forces and

wire magnetization. The results further optimized a prototype portable magnetic separator suitable for rapid sequestration of magnetic nano/micro-spheres from the human blood stream while accommodating necessary clinical boundary conditions.

Acknowledgement

This work was supported by the Defense Advanced Research Program Agency-Defense Science Office under contract 8C850, the Department of Energy under contract W-31-109-Eng-38, and The University of Chicago Brain Research and Cancer Research Foundations.

References

[1]C. Alexiou, R. J, R. Schmid, A. Hilpert, C. Bergemann, F. Parak and H. Iro, "In vitro and in vivo investigation of targeted chemotherapy with magnetic nanoparticles," J. Magn. Magn. Mater. **293**, 389-393 (2005).

[2]A. J. Rosengart, H. Chen, Y, Xie and M. D. Kaminski, "Magnetically guided plasminogen activator-loaded designed spheres for acute stroke lysis," Med. Hypotheses Res. **2**, 413-424 (2005).

[3]M. Saravanan, K. Bhaskar, G. Maharajan and K. S. Pillai, "Ultrasonically controlled resease and targeted delivery of diclofennac sodium via gelatin magnetic microspheres," Int. J. Pharm. **283**, 71-82 (2004).

[9]X. Liu, M. D. Kaminski, Y. Guan, H. Chen, H. Liu and A. J. Rosengart, "Preparation and Characterization of hydrophobic super paramagnetic magnetite gel," J. Magn. Magn. Mater. **306**, 248-253 (2006).

[10]H. Chen, A. D. Ebner, A. J. Rosengart, M. D. Kaminski and J. A. Ritter, "Analysis of magnetic drug carrier particle capture by a magnetizable intravascular stent 2: Parametric study with multi-wire two-dimensional model," J. Magn. Magn. Mater. **293**, 616-632 (2005).

[11]N. M. Orekhova, R. S. Akchurin, A. A. Belyaev, M. D. Smirnov, S. E. Ragimov and A. N. Orekhov, "Local prevention of thrombosis in animal arteries by means of magnetic targeting of aspirin-loaded red cells," Thromb. Res. **57**, 611-616 (1990).

[12]U. O. Hafeli, "Magnetically modulated therapeutic systems," International Journal of Pharmaceutics," **277**, 19-24 (2004).

[13]U. O. Hafeli, K. Gilmour, A. Zhou, S. Lee and M. E. Hayden, "Modeling of magnetic bandages for drug targeting: Button vs. Halbach arrays," J. Magn. Magn. Mater. (In press and available online).

[14]H. Chen, M. D. Kaminski, X. Liu, C. J. Mertz, Y. Xie, M. D. Torno and A. J. Rosengart, "A novel detoxification system based on nanoscale bioengineering and magnetic separation techniques," Med. Hypotheses (In press and available online).

[15]H. Chen, A. D. Ebner, J. A. Ritter, M. D. Kaminski, and A. J. Rosengart, "Magnetic dialysis for rapid blood detoxification: Part I. a theoretical study," J. Magn. Magn. Mater. (Submitted).

[16]I. Safarik, P. Mucha, and J. Pechoc *et al.*, "Separation of magnetic affinity biopolymer adsorbents in a Davis tube magnetic separator," Biotechnol. Lett. **23**, 851-855 (2001).

[17]G. B. Cotten, H. B. Eldredge, "Nanolevel magnetic separation model considering flow limitations," Sep. Sci. Technol. **37**, 3755 -3779 (2002).

[18]C. Hoffmann, M. Franzreb and W. H. Holl, "A novel high-gradient magnetic separator (HGMS) design for biotech applications," IEEE T. Appl. Supercond. **12**, 963-966 (2002).

[19]P. A. Augusto, P. Augusto and T. Castelo-Grande, "Magnetic shielding: application to a new magnetic separator and classifier," J. Magn. Magn. Mater. **272**, 2296-2298 (2004).

[20]N. Karapinar, "Magnetic separation of ferrihydrite from wastewater by magnetic seeding and high-gradient magnetic separation," Int. J. Miner. Process. **71**, 45-54 (2003).

[21]S. Nedelcu and J. H. P. Watson, "Magnetic separator with transversally magnetised disk permanent magnets," Miner. Eng. **15**, 355-359 (2002).

[22]V. Grano, N. Diano, M. Portaccio, U. Bencivenga, A. De Maio, N. De Santo, A. Perna, F. Salamino, and D.G. Mita, "The alpha(1)-antitrypsin/elastase complex as an experimental model for hemodialysis in acute catabolic renal failure, extracorporeal blood circulation and cardiocirculatory bypass," Int. J. Artif. Organs. **25**, 297-305 (2002).

[23]M.C. Yang and C.C. Lin, "*In vitro* characterization of the occurrence of hemolysis during extracorporeal blood circulation using a mini hemodialyzer," ASAIO J. **46**, 293-297 (2000).

[24]R.D. Swartz, M.G. Somermeyer and C.H. Hsu, "Preservation of plasma-volume during hemodialysis depends on dialysate osmolality," Am. J. Nephrol. **2**, 189-194 (1982).

[25]A. J. Rosengart and M. D. Kaminaki, in *Nanofabrication Towards Biomedical Applications*, edited by S. S. S. R. Kumar, J. Hormers, and C. Leuschner (WILEY-VCH Verlag GmbH & Co. KgaA, Weinheim, 2005).

[26]T.Y. Ying, S. Yiacoumi and C. Tsouris, "High-gradient magnetically seeded filtration," Chem. Eng. Sci. **55**, 1101-1113 (2000).

[27]G.D. Moeser, K.A. Roach, W.H. Green and T.A. Hatton, "High-gradient magnetic separation of coated magnetic nanoparticles," AIChE J. **50**, 2835-2848 (2004).

[28]A. Ditsch, S. Lindenmann, P. E. Laibinis, D. I. C. Wang and T. A. Hatton, "High-gradient magnetic separation of magnetic nanoclusters," Ind. Eng. Chem. Res. **44**, 6824-6836 (2005).

[29]J. Svoboda and V.E. Ross, "Particle capture in the matrix of a magnetic separator," Inter. J. of Mine. Processing. **27**, 75-94 (1989).

[30]R. Goleman, "Macroscopic model of particles' capture by the elliptic cross-section collector in magnetic separator," J. Magn. Magn. Mater. **272-276**, 2348-2349 (2004).

Fig. 1

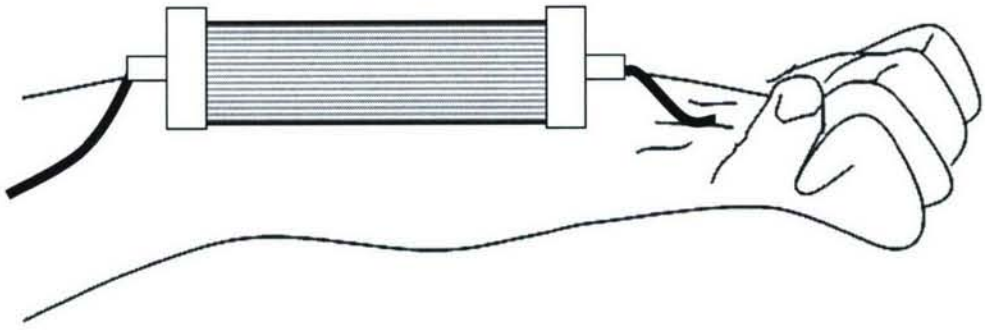

Fig.2

a)

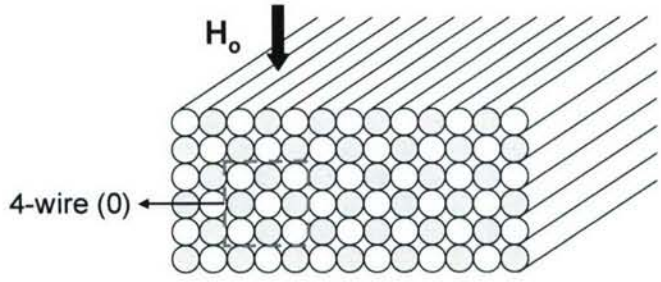

b)

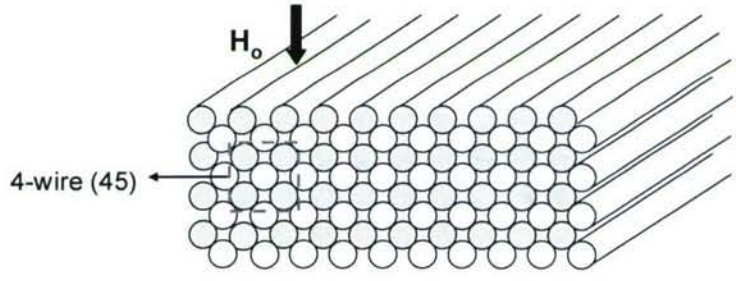

c)

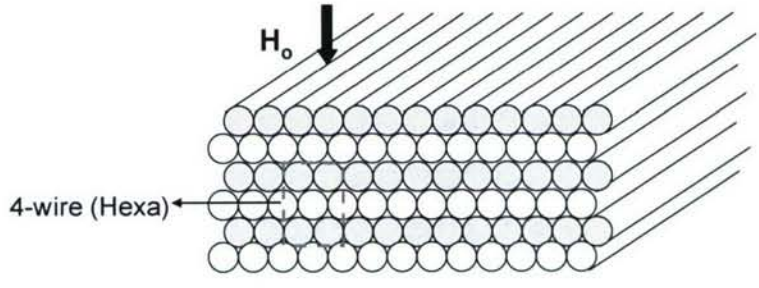

d)

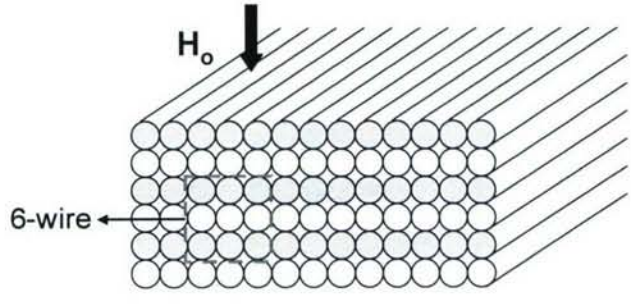

Fig. 3

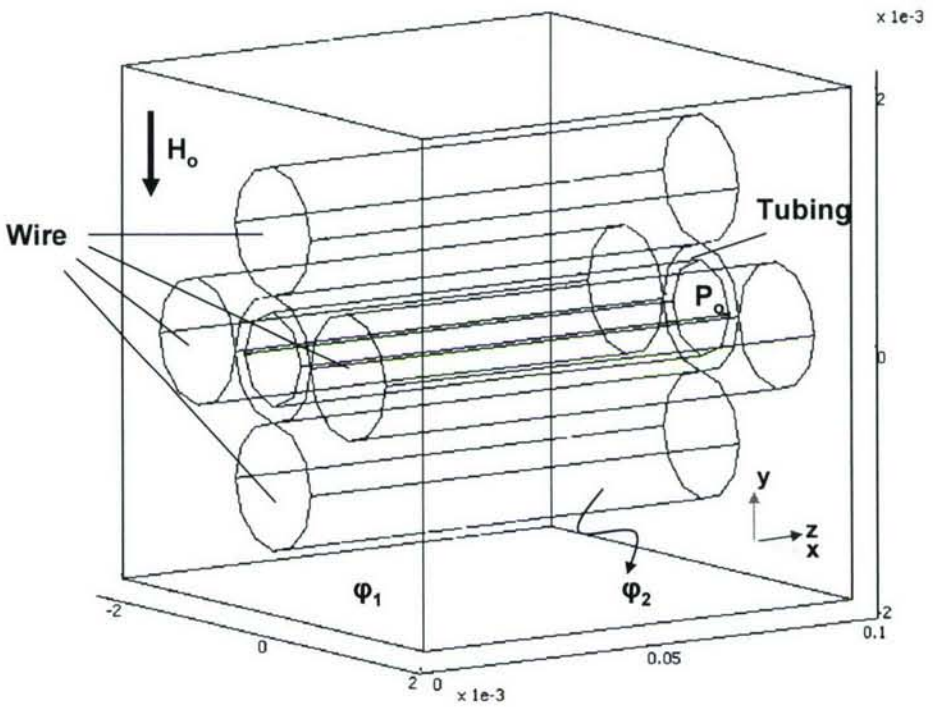

Fig. 4

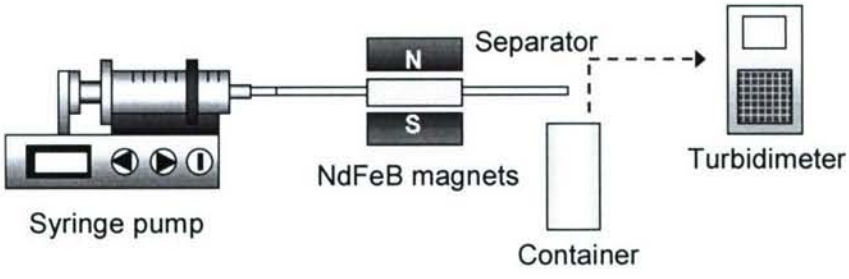

Fig. 5

a) 4-wire (0)

1) x=0

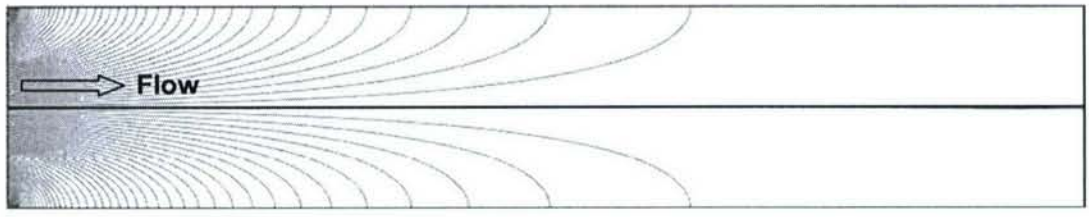

2) y=0

b) 6-wire

1) x=0

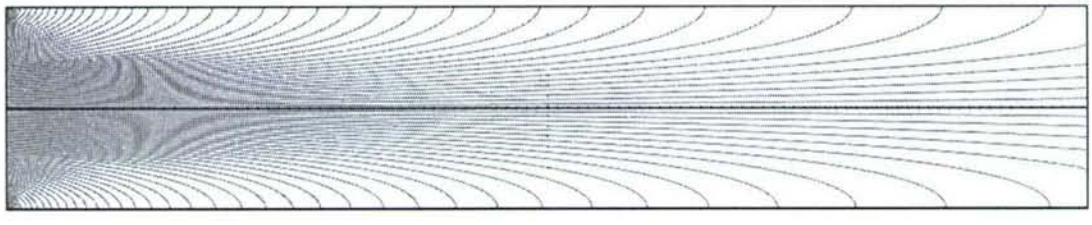

2) y=0

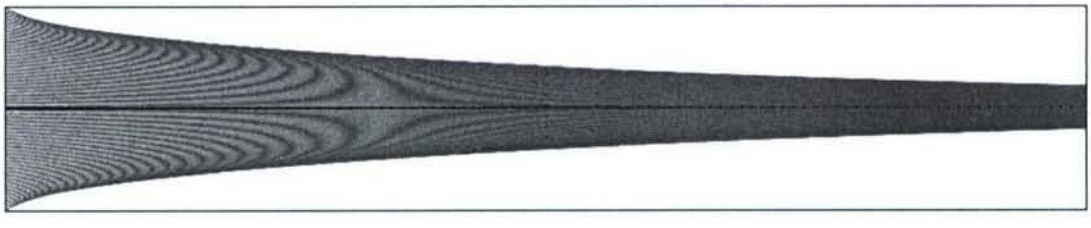

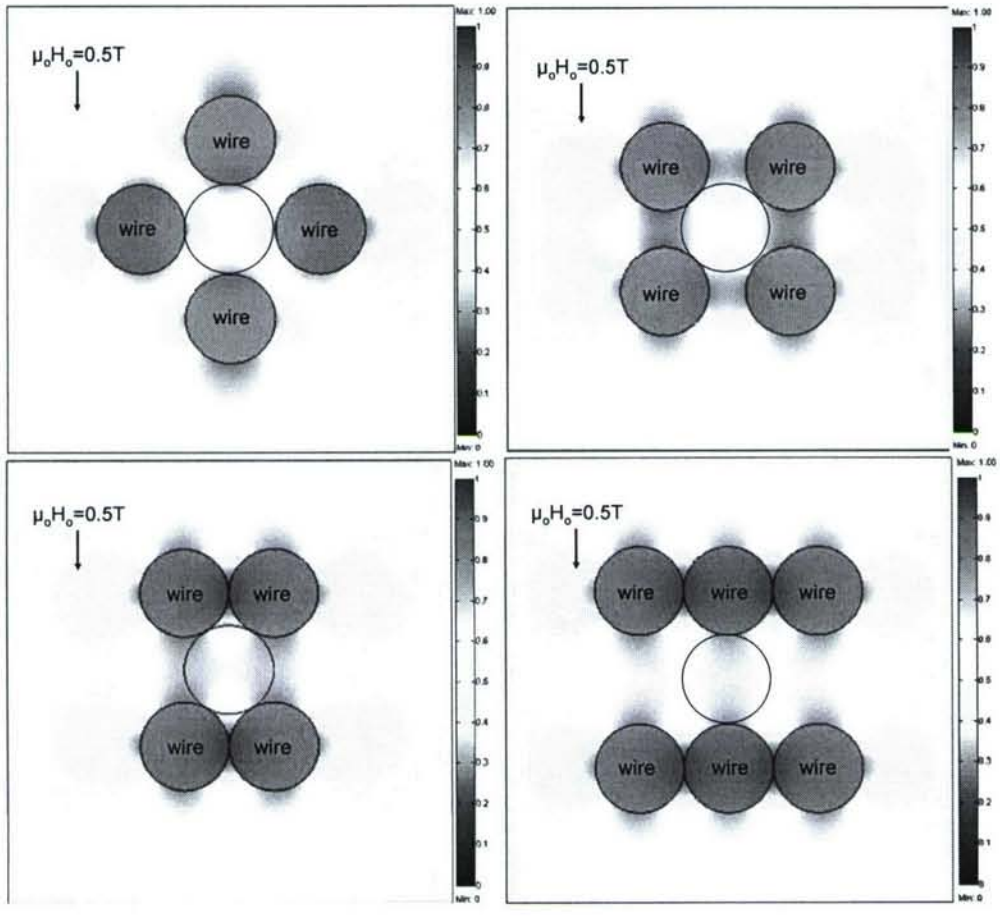
$\mu_o H_o$=0.5T
wire
wire
wire
wire
$\mu_o H_o$=0.5T
wire
wire
wire
wire
$\mu_o H_o$=0.5T
wire
wire
wire
wire
$\mu_o H_o$=0.5T
wire
wire
wire
wire
wire
wire

Fig.6

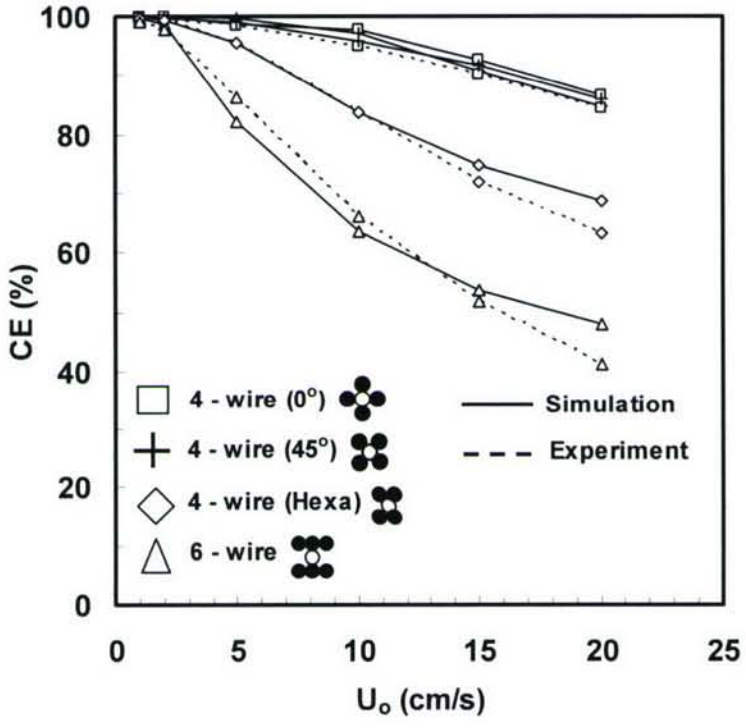
100
80
60
40
20
0
CE (%)
0
5
10
15
20
25
U_o (cm/s)
4 - wire (0°)
4 - wire (45°)
4 - wire (Hexa)
6 - wire
Simulation
Experiment

Fig.7

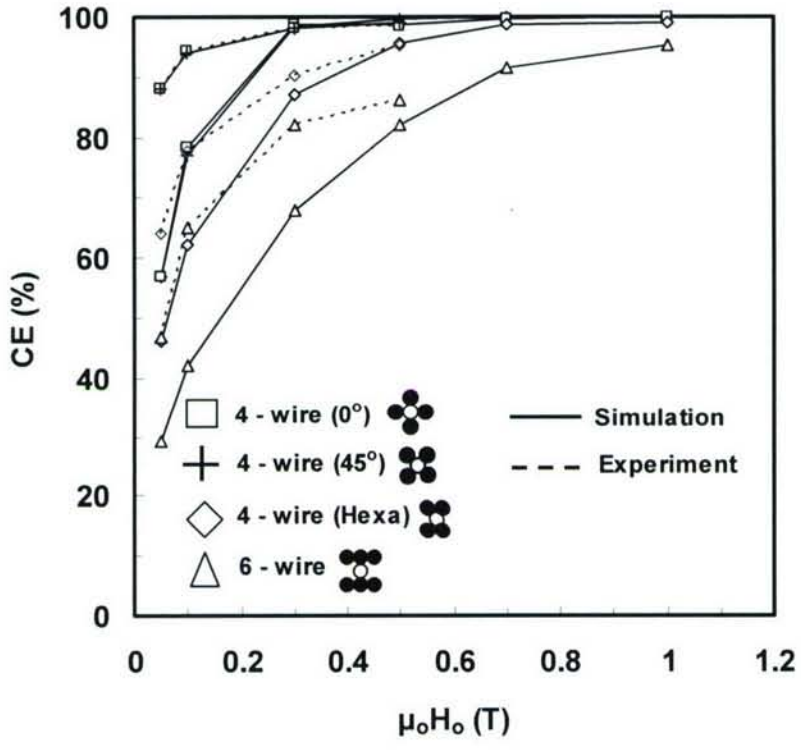
100
80
60
40
20
0
CE (%)
0
0.2
0.4
0.6
0.8
1
1.2
μoHo (T)
4 - wire (0°)
4 - wire (45°)
4 - wire (Hexa)
6 - wire
Simulation
Experiment

Fig. 8

a)

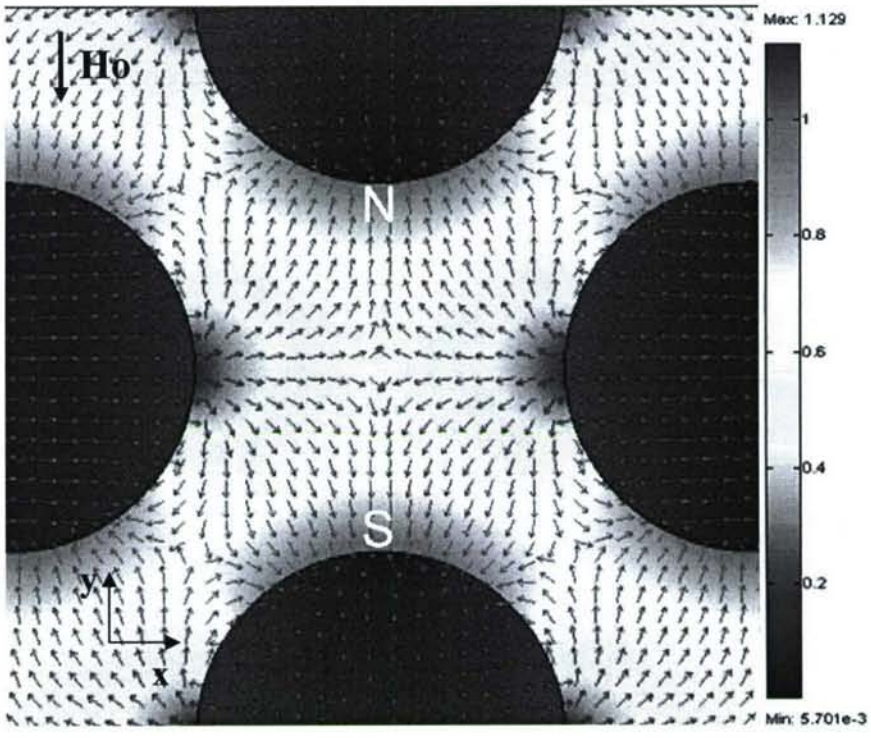
Ho
N
S
y
x
Max: 1.129
1
0.8
0.6
0.4
0.2
Min: 5.701e-3

b)

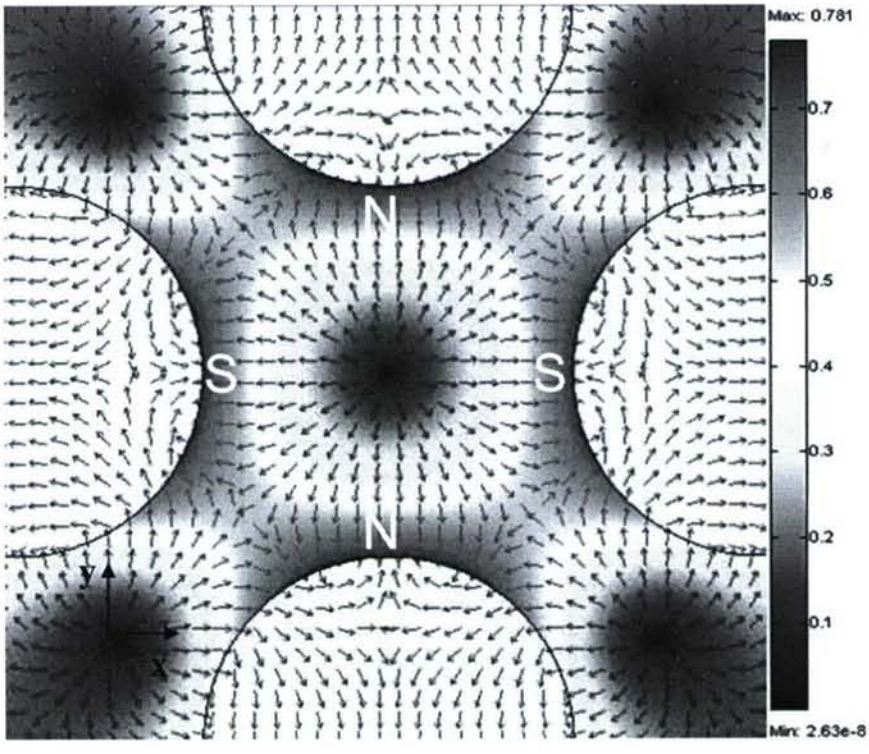
N
S
S
N
y
x
Max: 0.781
0.7
0.6
0.5
0.4
0.3
0.2
0.1
Min: 2.63e-8

Fig. 9

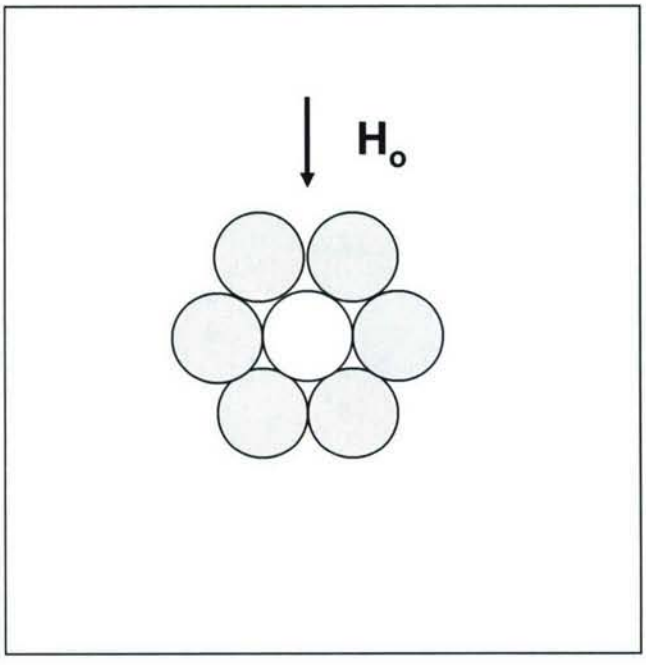

Captions

1. Conceptual sketch of separation of toxin-bound magnetic nanospheres from human blood using a portable magnetic separator device.
2. The possible configuration designs of the magnetizable wires (dark-colored) and tubing (light-colored) in the separator. Four basic configuration units (in dash lines) were named from the designs: 1) 4-wire (0); 2) 4-wire (45), 3) 4-wire (Hexa) and 4) 6-wire.
3. An example of the schematic of magnetic separator units (3-D) investigated in the current study.
4. Experimental set-up.
5. The trajectories of magnetic spheres in the tubing for the a) 4-wire (0) configuration and b) 6-wire configuration on the planes of 1) x = 0 and 2) y = 0 (U_o = 5 cm/s and $\mu_o H_o$ = 0.5 T). The fluid and spheres flows from left to right.
6. Comparison between numerical and experimental results at different flow velocities ($\mu_o H_o$ = 0.5 T).
7. Comparison between numerical and experimental results at different applied field strengths (Uo = 5 cm/s).
8. Comparison between a) 4-wire (0) configuration design and b) quadrupole magnetic field design (from COMSOL Multiphysics simulation). The color presents the intensity of magnetic field density and the arrows indicate the direction of magnetic force.
9. A hexagonal configuration design unit of the magnetizable wires (dark-colored) and tubing (light-colored) in the separator.

Table I. Values and ranges of the parameters used in the model and experiments.[a]

Parameters	Units	Values
Fluid density, ρ	kg/m^3	1000
Fluid viscosity, η	kg/(m s)	1.0×10^{-3}
Fluid temperature, T	K	298.15
Mean fluid velocity, U_o	cm/s	1.0 – 20.0, <u>5.0</u>
Tube inner radius, R_i	mm	0.375
Tube outer radius, R_o	mm	0.500
Tube wall thickness, h	mm	0.125
Tube length, L_t	mm	100
Sphere radius, R_p	nm	850
Sphere magnetic material[b]		magnetite
Magnetite radius, R_{fm}	nm	5
Sphere magnetite mass fraction, $x_{fm,p}$		12.85%
Sphere polymer density, ρ_{pol}	kg/m^3	1050
Wire material[b]		SS 430
Wire radius, R_w	mm	0.5
Wire length, L_w	mm	100
Magnetic field flux density, $\mu_o H_o$	T	0.05 – 1.0, <u>0.5</u>

[a]Base case conditions underlined

Preparation and Characterization of Hydrophobic Superparamagnetic Magnetite Gel

Xianqiao Liu[a], Axel J. Rosengart[a]*, Yueping Guan[b], Haitao Chen[a], Michael D. Kaminski[c] and Sandra Guy[a]

[a]Department of Neurology and Surgery (Neurosurgery), The University of Chicago and Pritzker School of Medicine, Chicago, IL, USA
[b]Laboratory of Separation Science and Engineering, Institute of Process Engineering, Chinese Academy of Sciences, Beijing, China
[c]Chemical Engineering Division, Argonne National Laboratory, Argonne, IL, USA

Abstract

The present study deals with the preparation and analysis of highly concentrated, hydrophobic oleic acid-coated magnetite gel. By contrast to conventional techniques to prepare magnetic fluid, herein the oleic acid was introduced as a reactant during the initial crystallization phase of magnetite which was obtained by the co-precipitation of Fe(II) and Fe(III) salts by addition of ammonium hydroxide. The resulting gelatinous hydrophobic magnetite was characterized in terms of morphology, particle size, magnetic properties, and crystal structure. The magnetic gel exhibited superparamagnetism at room temperature and could be well dispersed both in polar and nonpolar carrier liquids.

Keywords: Magnetic gel; preparation; magnetite; superparamagnetism; FT-IR spectroscopy

1. Introduction

Magnetic iron oxide nanoparticles and their dispersions in various media called magnetic fluids (ferrocolloids) have long been of scientific and technological interest since the 1960s. Owing to their unique properties in a magnetic field they are actively used in different industrial, technical, as well as biological and medical applications over the past three decades [1-3]. The magnetic fluids based on magnetite and mineral oils or organic solvents are conventionally prepared by alkaline hydrolysis of ferrous and ferric salts. The magnetite obtained is stabilized by surfactants[4,5].

* To whom correspondence should be addressed. Tel.: +1773 702 2364. Fax: +1773 834 4612.
E-mail: arosenga@neurology.bsd.uchicago.edu

The oleic acid is usually used as a surfactant, which forms the waterproofing shell around the magnetite particles. The treatment of magnetite by oleic acid is the most complex and important stage of the magnetic magnetite fluid preparation. This stage of the magnetic fluids preparation determines its service properties [6]. In conventional techniques to prepare magnetic fluids, the oleic acid was often served as surfactant for the magnetite particles stabilization after the complete crystallization of magnetite precipitate [7]. However, concentrating the magnetic fluids to increase the magnetization and their content in some encapsulation treatment for biomedical applications proved to be very difficult. It is also difficult to incorporate high concentrations of hydrophilic magnetite into hydrophobic polymer such as poly (lactic acid) (PLA), poly (lactide-co-glycolide) (PLGA) etc [8]. In this connection, the investigations of the novel methods of highly concentrated hydrophobic magnetite preparation are very important in practical terms.

In this study we report a simple and efficient method to prepare a hydrophobic oleic acid-coated magnetite gel. In contrast to the conventional methods, in our technique, the oleic acid, as a reactant, was added immediately after the formation of magnetite, simultaneously with the crystal growth. It was proposed that the oleic acid will efficiently coat the Fe_3O_4 crystal at the growth stage and will create a highly concentrated hydrophobic magnetite gel. We characterized the magnetite gel in terms of their morphology, particle size, magnetic properties, structure and hydrophobicity/hydrophilicity with a transmission electron microscope (TEM), vibrating sample magnetization (VSM), Powder X-ray diffraction (XRD) and Fourier Transform Infrared (FTIR) spectrometer.

2. Experimental

2.1. Materials

Ferrous chloride tetrahydrate (99%), ferric chloride hexahydrate (99%), ammonium hydroxide (25 wt% NH_3 in water), oleic acid (90%), hexane (95%), sodium dodecylbenzene sulfonate (SDS) were purchased from Sigma-Aldrich (St. Louis, MO) and used without any further purification. Water was deionized and deoxygenated prior to use.

2.2. Preparation of magnetic magnetite gel

The magnetic magnetite gel was prepared by the following procedure: 11.60 g $FeCl_3 \cdot 6H_2O$ and 4.30 g $FeCl_2 \cdot 4H_2O$ were dissolved in 400 ml deionized water under nitrogen gas with vigorous stirring at 90°C. 15 ml 25 wt% $NH_3 \cdot H_2O$ was added to the solution. Then 9 ml oleic acid was added dropwise into the suspension. After several minutes, the upper solution became colorless and the tar-like black gel precipitated. The magnetic gel was thoroughly washed with ethanol and deionized water several times to pH 7.0.

The above magnetic gel was directly dispersed in organic carrier liquids such as hexane, styrene, ethyl acetate to form stable organic magnetic fluids. At the same time, a stable aqueous magnetic fluid could be formed by dispersing magnetic gel into water with addition of several drops of ammonium hydroxide or SDS.

2.3. Characterization

Transmission electron microscope (TEM, Hitachi 8100) was used to measure the morphology and size of magnetite nanoparticles. The samples for TEM analyses were obtained by placing a drop of the diluted hexane solution onto a 300 mesh carbon coated copper grid and evaporated in air at room temperature. TEM pictures were taken at an accelerating voltage of 200 kV. A vibrating sample magnetometer (VSM, Digital Measurement System, model 155) was employed to investigate the magnetic properties of samples by measuring the magnetization as a function of magnetic field intensity. Powder X-ray diffraction (Philips Wide Angle Goniometer, Cu Kα) was used to study the crystal structure of samples. The FTIR spectra were recorded in the absorbance mode on a Fourier transform infrared spectrophotometer (FTIR, Bruker, Vecter 22). The magnetic gel was dispersed in carbon tetrachloride to form a colloid solution and the spectra were measured in CaF_2 cells.

3. Results and Discussion

3.1 magnetic Fe_3O_4 gel

Fig. 1(A) shows the TEM image of the naked Fe_3O_4 nanoparticles with an average size of 15 nm by statistics; and Fig. 1(B) TEM image reveal that in hexane the magnetite gel was dispersed relatively independently with an average diameter of 8 nm. It is well known that the magnetite nanoparticles prepared by co-precipitation have extensive hydroxyl groups on the surface by contact with the aqueous phase. Since the surface-to-volume ratio is very large, the surface hydroxyl groups reacted readily with the carboxylic acid head groups of the oleic acid molecule at a temperature of 90°C. The oleic acid added was first adsorbed chemically on the Fe_3O_4 surface to form the first coating layer of oleic acid molecule through the "esterification" or electrostatic interaction between their carboxylic acid head groups and the hydroxyl groups shown as:

Then the subsequent oleic acid molecule was physically adsorbed on the first coating layer to form a waterproofing shell. As a result, a tar-like black gel was precipitated spontaneously at the end of reaction. Compared with the naked magnetite, the oleic acid-coated Fe_3O_4 gel are dispersed independently and the particle size are even smaller than their naked counterpart, which is probably because magnetite crystal growth was restrained by the oleic acid molecule coating.

In the conventional method, an extensive base was usually used to form magnetite precipitate and oleic acid was added as a surfactant for the stabilization of magnetite magnetic fluid by forming oleate directly since oleic acid has the highest affinity to the surface of superfine

magnetite among other surfactants [4]. However, it is difficult to disperse high concentrations of such magnetic fluids into droplets of hydrophobic monomers. Thus, the magnetite content in the final polymer sphere is usually limited [9,10]. In the present work, the highly concentrated hydrophobic magnetite gel was obtained by adjusting the amount of ammonium hydroxide and oleic acid, and the time of oleic acid addition as well. Regardless of the size of particles, the key to the success of making such hydrophobic magnetite gel is to add an appropriate amount of ammonium hydroxide and oleic acid so that the final solution remain neuter and the magnetite gel precipitated spontaneously. This protocol produced highly concentrated hydrophobic magnetite gel for high quality magnetic fluid preparation as well as magnetic polymer encapsulation.

3.2. Magnetic properties

The magnetic properties of the magnetic magnetite gel were tested by VSM magnetometer as shown in Fig. 2. The sample shows typical superparamagnetic behavior without any hysteresis loop at room temperature. The origin of superparamagnetism can be explained as follows. Due to small particle size, anisotropy energy is less than the thermal agitation energy of the ions, so magnetized direction is no longer fixed in an easy magnetized direction, and the movement of the ions is random. Consequently, the sample would display a superparamagnetic nature like a paramagnetic body [11]. For superfine magnetically ordered particles, there exists a critical size (D_p) below which the granules can acquire only single magnetic domains even in a zero magnetic field. It was reported that the critical size of magnetite ($D_p Fe_3O_4$) at room temperature was about 25nm based on the theoretical calculation [12].When the particle size is less than the D_p, magnetic particles would lose ferromagnetic or subferromagnetic properties which are inherent in the bulk materials, and exhibit a remanent superparamagnetic state with no hysteresis. When this occurs, the values of the remanence (Mr) and coercivity (Hc) of the sample is zero. The magnetization curve of the sample reversibly goes through the zero point.

It was indicated from TEM image that the particle size of gelatinous magnetite is about 8nm, much less than the D_p. As expected, the magnetization curves versus applied fields exhibited no hysteresis and the magnetization curves go through the zero point and overlap together as shown in Fig. 2. All of these manifest the superparamagnetic nature of the samples at room temperature.

3.3. XRD and FTIR analysis

Fig. 3 is the X-ray diffraction patterns of the oleic acid-coated magnetite gels. It is well known that Fe_3O_4 can be oxidized to γ- Fe_2O_3, which can be further transformed into α- Fe_2O_3 at higher temperature. The diffraction peaks at (113), (210), (213), and (210) are the characteristic peaks of γ- Fe_2O_3 and α- Fe_2O_3 respectively [13]. The standard Fe_3O_4 crystal with a cubic spinel structure has distinct diffraction peaks: (110), (220), (311), (400), (422), (511), and (440). The XRD of magnetite gel samples shown in Fig. 3 matches the standard Fe_3O_4 powder diffraction very well. The position and relative intensity of all diffraction peaks are identical with standard spectra for bulk magnetite, except for the broadening of the peaks. Therefore, it can be concluded that the magnetite dispersed in the magnetic gel are also of the inverse cubic spinel structure. No peaks were detected which could be assigned to impurities such as γ- or α-ferric oxide.

Fig. 4 shows the FTIR spectra of the magnetite gel dispersed in carbon tetrachloride. The broad bands with a maximum at 580 cm^{-1} correspond to vibrations of the Fe-O bonds in the crystalline lattice of magnetite. Since the magnetic gel was thoroughly washed and the pH value of the final solution was 7.0, no free oleate ($-COO^-$) will exist in the sample solution. In conventional magnetic fluid in which the oleic acid molecule is adsorbed as surfactant, the adsorption will result in some changes in the spectra of the surfactant. For example, the adsorption bands at 1710 cm^{-1} (oleic acid molecule), which are assigned to stretching vibrations of C=O of the carboxyl group, disappeared in the spectrum of the final magnetic fluid [4]. In contrast to conventional magnetic magnetite fluid spectra, an obvious adsorption band at 1710 cm^{-1} appeared in the sample spectra, which indicated the presence of oleic acid molecules. At the same time, the bands at 1430

cm^{-1} and 1590 cm^{-1} appeared, which corresponding to the symmetric and antisymmetric stretching vibration of oleate ($-COO^-$). All of these indicate that both oleic acid and oleate exist in the magnetic gel, which is different from conventional magnetic fluid.

3.4. Possible mechanism for the formation of magnetite gel

The mechanism leading to the formation of magnetite gel in the reactions presented is not yet clear. Evidence suggests that the co-precipitation of Fe(III) and Fe(II) salt intermediates occurs, followed by crystallization. During this initial process, the oleic acid molecule was chemically bound to the surface of Fe_3O_4 particles. Consequently, the iron oxide nanoclusters were coated with a well-organized primary oleic acid molecule. Then, the excess oleic acid was adsorbed on the primary layer of the oleic acid-coated magnetite to form a hydrophobic shell through the hydrophobic interaction between the subsequent oliec acid molecule and the hydrophobic tail of oleate adsorped on Fe_3O_4 already. Finally, the single layer oleic acid-coated magnetite and extensive oleic acid molecules condensed to form magnetic gel and precitated spontaneously.

The synthesized highly concentrated hydrophobic magnetite gel could be easily mixed with nonpolar carrier liquids such as hexane, styrene, ethyl acetate and kerosene. During this process, extensive oleic acid molecules will disperse into oil and the gel was transferred to colloid by forming single layer oleic acid-coated Fe_3O_4 dispersions shown in Fig. 5. The dispersions showed properties of the so-called ferrofluid. It is very interesting that an aqueous magnetic fluid could also be obtained by dispersing the magnetic gel into water with the addition of several drops of ammonium hydroxide which leads to the formation of ammonium oleate as a surfactant. The possibe mechanism is also proposed schematically in Fig. 5.

In organic solvent, the magnetite gel has less oleate outside the primary layer (tightly chemiadsorbed). This point is important to the discussion of dispersibility of the particles. The issue of particle dispersibility in solvents is a major criterion for various practical purposes (e.g. stable ferrofluids) and for basic studies such as understanding interparticle magnetic interactions,

where it is important to obtain well-isolated particles. In aqueous magnetic fluid, the magnetite gel were water dispersible as a consequence of the polar groups (oleate) on the surface of the primary oleic acid layer (chemiadsorbed), which enables the formation of a full polar shell that makes the particle surface hydrophilic. A similar structure has been reported on the aqueous decanoic acid-coated magnetite magnetic fluid [14].

4. Conclusions

A highly concentrated hydrophobic magnetite gel was prepared on the basis of co-precipitation with some efficient modifications. The magnetic gel prepared consists of Fe_3O_4 nanoparticles, chemically adsorbed oleate, and oleic acid molecule. They exhibit superparamagnetism at room temperature and could be well dispersed directly into nonpolar or weakly polar hydrocarbon solvents such as hexane or ethyl acetate. The hydrophobic magnetic gel can also be made hydrophilic by adjusting the pH value of the medium or mixing with a bipolar surfactant SDS, allowing preparation of aqueous nanoparticle dispersions. These magnetic gel and their dispersions, in various media, have great potential in magnetic separation and biomagnetic applications.

Acknowledgments

This work is supported by the Defense Advanced Research Agency-Defense Science Office under contract 8C850, the Department of Energy under contract W-31-109-Eng-38, and the University of Chicago Brain Research and Cancer Research Foundations.

Reference:

[1] J.M. Perez, L. Josephson, R. Weissleder, ChemBiochem 5(2004) 261.

[2] S.M. Moghimi, A.C. Hunter, J.C. Murray, FASEB J. 19(2005) 311.

[3] M. Shinkai, J. Biosci. Bioeng. 94(2002) 606.

[4] V.V. Korolev, A.G. Ramazanova, A.V. Blinov, Russ. Chem. Bull. 51(2002) 2044.

[5] E. Blums, A. Cebers, M.M. Maiorov, Magnetic Fluids, Walterde Grvoyter, Berlin, 1997

[6] A.L. Kholmetskii, S.A. Vorobyova, A.I. Lesnikovich, V.V. Mushinskii, N.S. Sobal, Mater. Lett. 59(2005) 1993.

[7] Y. Sahoo, H, Pizem, T, Fried, D.Golodnitsluy, L. Burstein, C.N. Sukenik, G. Markolich, Langmuir 17(2001) 7907.

[8] R.H. Müller, S. Maassen, H. Weyhers, F. Specht, J.S. Lucks, Int. J. Pharm. 138(1996) 85.

[9] Z.L. Liu, Z.H. Ding, K.L. Yao, J. Magn. Magn. Mater. 265(2003) 98.

[10] P.A. Dresco, V.S. Zaitsev, R.J. Gambino, B. Chu. Langmuir 15(1999) 1945.

[11] C.P. Bean, J.D. Livingston, J. Appl. Phys. 30(1959) 120.

[12] J. Lee, T. Isobe, M. Senna, J. Colloid Interface Sci. 177(1996) 490.

[13] S. Sun, H. Zeng, D.B. Robinson, S. Raoux, P.M. Rice, S.X. Wang, G. Li, J. Am. Chem. Soc. 126 (2004) 273.

[14] L. Shen, P.E. Laibinis, T.A. Hatton, J. Magn. Magn. Mater. 194(1999) 37.

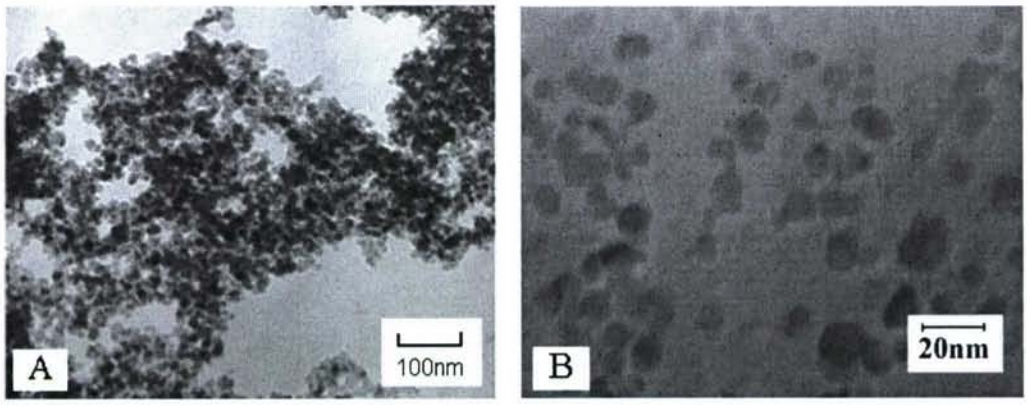

Fig.1. TEM of naked magnetite nanoparticles (A) and oleic-acid coated Fe_3O_4 gel (B)

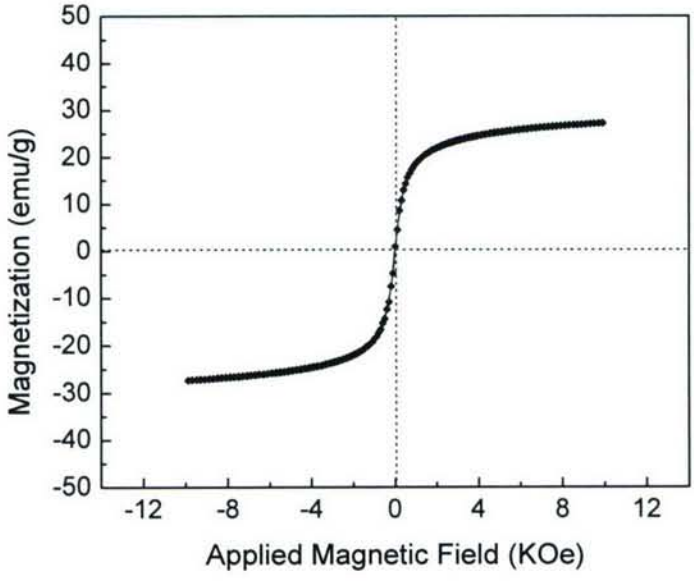

Fig.2. VSM magnetization curve of oleic acid-coated Fe_3O_4 gel.

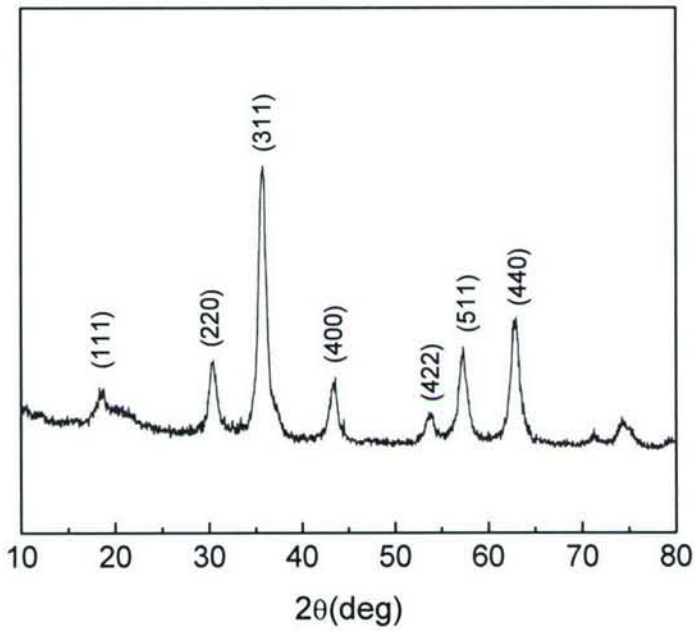

Fig.3. XRD patterns of oleic acid-coated magnetite gel.

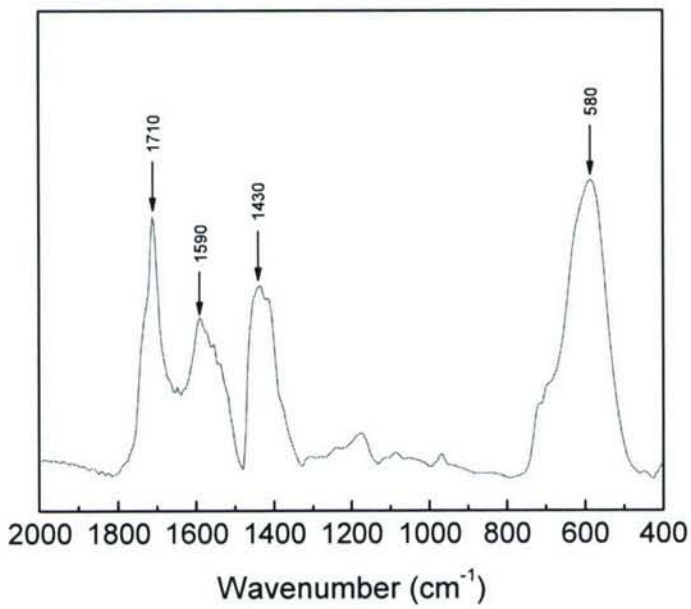

Fig.4. FTIR spectra of magnetic Fe_3O_4 gel in an organic solvent (CCl_4).

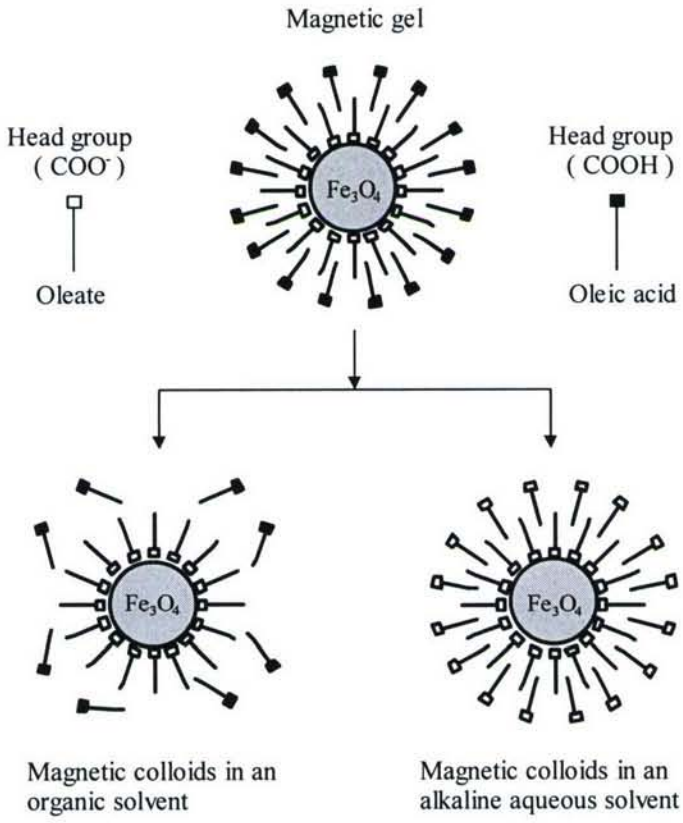

Fig.5. Possible mechanism of magnetic Fe_3O_4 gel dispersed in polar and nonpolar solvent.